STUDY THE ELECTRONIC AND OPTICAL PROPERTIES OF $Rb_2NaScCl_6$ DOUBLE PEROVSKITE FOR THE APPLICATION OF ENERGY CONSUMPTION
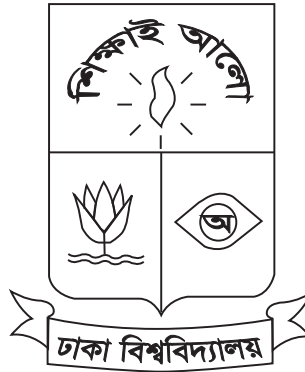
COURSE TITLE: THESIS
COURSE CODE: TPG-599

SUBMITTED BY

REGISTRATION NUMBER: 2016-414-723
EXAM ROLL: 106711
ACADEMIC YEAR: 2020-21

THIS THESIS IS SUBMITTED TO DEPARTMENT OF
THEORETICAL PHYSICS, UNIVERSITY OF
DHAKA IN PARTIAL FULFILLMENT OF
THE REQUIREMENT FOR THE
DEGREE OF M.S. IN
THEORETICAL PHYSICS

4 JULY, 2023

Abstract

Recent energy deficits have influenced an intensification of demand for renewable energy sources. The utilization of these energy sources necessitates the availability of substances that possess the capability of absorbing visible wavelengths of light. The electronic and optical properties, along with the structure stability of $Rb_2NaScCl_6$, a double perovskite devoid of toxicity, were determined in our study. The DFT calculation utilizing the WIEN2k program is implemented in our study. The stability and legality of the structure being an ideal cubic symmetry along with space group Fm$\bar{3}$m have been determined through the utilisation of the tolerance factor and octahedral factor. The precise value for the band-gap is identified as being 3.9 electron volts, while the absorption coefficient has been observed to fall within the ultra-violet range. The compound's simulated properties were analysed under different pressure conditions. Both electronic and optical properties shows a significant change under different pressure. The results show that the band-gap got broader up to 20 GPa, but then it started to get smaller as the pressure went up. Additionally, there was a shift in absorption from the ultra-violet to visible range of wave length as pressure increased over 20 GPa. With appropriate modification, the material exhibits promising potential for utilization in diverse sectors, particularly in the realm of new energy production applications.

Acknowledgements

Contents

Contents

Contents

List of Figures

List of Tables

List of Abbreviations

DFT   :   Density Functional Theory

VB   :   Valance Band

CB   :   Conduction Band

LDA   :   Local density approximation

DOS   :   Density of States

eV   :   Electro volt

LAPW   :   Linearized Augmented Plane Wave

PDOS   :   Partial density of states

EEL   :   Electron energy loss

GGA   :   Generalized Gradient Approximation

UV   :   Ultra-violet

LSDA   :   Local Spin Density Approximation

LEDs   :   Light Emitting Diodes

XC   :   Exchange-correlation

STUDY THE ELECTRONIC AND OPTICAL PROPERTIES OF $Rb_2NaScCl_6$ DOUBLE PEROVSKITE FOR THE APPLICATION OF ENERGY CONSUMPTION

<div align="right">

Chapter 1

</div>

Introduction

People are flocking toward new technologies as civilisation advances. The majority of technological advancements are dependent on the uninterrupted supply of energy. Our energy resources are becoming more and more scarce. Future society will need energy sources that are renewable and favorable to the environment. The power sector has identified renewable energy sources as the way forward since they can replace traditional fossil fuels with carbon-based counterparts while supplying an unbroken flow of electricity [1, 2]. Hence, success in the field of renewable energy is closely related to the goal of a carbon-neutral energy economy. Technologies including solar cells, water-splitting, and thermoelectricity have got the attraction to scientific association recently. For those technologies, various compounds are being developed while taking efficiency, usability, and environmental impact into consideration. Due to its effectiveness and multidimensional applications, founded both theoretically and computationally, double perovskite is currently one of them.

Throughout the course of the last ten years, double perovskite has garnered significant interest from both a theoretical and an experimental perspective. In addition to its practical applications, double perovskite systems offer insight into the physics behind the emergence of functional characteristics. Double perovskite materials have gained a lot of curiosity lately due to its potential applications in a variety of

Introduction

disciplines, including LEDs (light-emitting diodes), photovoltaic cell, sensors, fuel cells, LASERS, thermoelectricity, catalysis, radiation detectors, and a wide variety of other fields and industries [3–9].

The investigation of double perovskite was initiated in the vicinity of the 1950s [10]. The term double perovskite comes from from the name perovskite. A double perovskite exhibit the recurrence of perovskite unit cell. Solar cells and other photovoltaic technologies work well with lead-based perovskites [11, 12]. Lead perovskite solar cells are used a lot in photovoltaic because they are easy to make and have a high power conversion efficiency of more than 20%. Unfortunately, lead had to be replaced because it was dangerous and unstable [13]. The double perovskites work well in a variety of fields and have a lot of stability with non-toxic materials that are good for the environment. Lead-free double perovskites, such as Rb_2ScInI_6, $Rb_2AgCrCl_6$, $Cs_2AgBiBr_6$ et cetera have demonstrated high efficiencies in renewable technology like photovoltaic cells [14–16]. Several double perovskites such as Gd_2ZnTiO_6:Mn^{4+}, $NaLaMgWO_6$:Eu^{3+}, Ca_2LaSbO_6:Sm^{3+} exhibit the potential for use in optical devices such as LEDs when doped [17–19]. These materials exhibit a variety of magnetic behaviors, including ferromagnetism, antiferromagnetism and ferrimagnetism, depending on the metal ions. For example, La_2NiMnO_6 and Sr_2FeMoO_6 are ferromagnetic and exhibit magneto-resistance, making them promising candidates for spintronic applications [20, 21]. Some double perovskite compounds exhibit superconducting properties at low temperatures. For instance, double-perovskite bismuth oxides have demonstrated high efficiency in the field of superconductivity [22].

To understand the electronic, optical and other characteristics of a double perovskite is essential to comprehend its usefulness in various fields. However, conducting experimental research requires a significant amount of resources and financial support. Density functional theory based computational investigations can point the way for experimental endeavours and, in many instances, provide a greater insight into the synthesized, associated features, and application of materials. Electronic, optical, elastic, thermoelectronic and many other property can be determined based on density functional theory [23–26] accurately, and several observation shows its validity by comparing with experimental data.

Introduction

Our study determines the electronic and optical characteristics of $Rb_2NaScCl_6$ double perovskite compound. To do our calculation, we use the WIEN2k program, which uses the first principle density functional theory. We examine the numerous ways we might use our compound, like for application of energy consumption.

1.1 Structure Description

The general structure of double perovskites is $A_2B'B''C_6$, where C could be halogen or oxygen molecule [27, 28]. Here A is an alkaline-earth or rare-earth ion. The one or both cation sites B' and B'' are occupied with transition-metal. The structure of perovskite compounds has similarities with the structure of double perovskite having ABC_3 crystal structures. Intervening oxygen/halogen bridges every B' and B'' atom pair, thus forming alternating $B'C_6$ and $B''C_6$ octahedra. This type of compound most probably forms perfectly cubic structures with the space group $Fm\bar{3}m$ (space group no: 225).

In our study, we work with $Rb_2NaScCl_6$ double perovskite compound. The polyhedral structure representation of $Rb_2NaScCl_6$ double perovskite provided in figure 1.1.
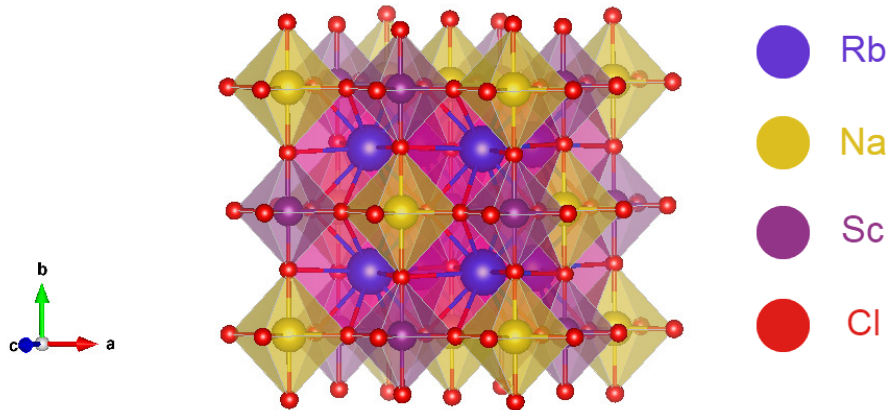
Figure 1.1: Polyhedral presentation of the crystal structure $Rb_2NaScCl_6$

The structure contains 40 atoms, 143 lattice points, 258 bonds and 35 polyhedral. In this a single unit cell, the A sites are filled with 8 rubidium (Rb) atoms, the B'

Introduction

and B$''$ sites are filled with 4 sodium (Na) and 4 scandium (Sc) atoms. There are 24 chlorine (Cl) atoms which forms octahedra with Na and Sc atoms. The volume of the unit cell is 1173.548970 Å^3. The crystal structure is a cubic structure with space-group 225 Fm$\bar{3}$m. The stability of our compound is demonstrate with tolerance factor (τ) as well as octahedral factor (μ). And these components can be represents by the following equations [29, 30]:

$$\tau = \frac{T_a + T_o}{\sqrt{2}(\frac{T_{b'} + T_{b''}}{2}) + T_o} \tag{1.1}$$

$$\mu = \frac{T_{b'} + T_{b''}}{2T_o} \tag{1.2}$$

Here, T_a, $T_{b'}$, $T_{b''}$, and T_o represents the ionic radius of A, B$'$, B$''$ and C components of double perovskite. For a stable double perovskite, the value of tolerance factor is between 0.71 to 1, while the value of octahedral factor is between 0.42 to 0.75 [31, 32]. Furthermore, research has demonstrated that materials exhibiting a tolerance factor ranging from 0.89 to 1.00 indicate a cubic structure [33]. For the material Rb$_2$NaScCl$_6$ double perovskite, the ionic radius of Rb, Na, Sc, Cl is used 1.72 Å, 1.02 Å, 0.745 Åand 1.81 Årespectively. The values of the tolerance factor and octahedral factor have been determined to be 0.927 and 0.487 respectively. The value ensures that the material exhibiting the form of cubic structure having the space group of Fm$\bar{3}$m, which corresponds to space group number 225. The atom's coordination and lattice parameters have displayed in table 1.1 and 1.2 correspondingly.

Table 1.1: Table of lattice parameters

a (Å)	b (Å)	c (Å)	alpha (α)	beta (β)	gamma (γ)
10.54793	10.54793	10.54793	90.0000°	90.0000°	90.0000°

Table 1.2: Position of atoms

ATOM	NUMBER	X	Y	Z
Rb	1	0.75000	0.25000	0.25000
Rb	2	0.25000	0.75000	0.75000
Na	1	0.00000	0.00000	0.00000
Sc	1	0.50000	0.00000	0.00000
Cl	1	0.50000	0.23704	0.00000
Cl	2	0.50000	0.76296	0.00000
Cl	3	0.76296	0.50000	0.00000
Cl	4	0.23704	0.50000	0.00000
Cl	5	0.00000	0.50000	0.23704
Cl	6	0.00000	0.50000	0.76296

1.2   Organization of Chapters

Apart from this introductory chapter, this thesis contains four other chapters. We will discuss about electronic and optical properties of a substance in chapter two. After that, chapter three discusses density functional theory. The renowned Schrödinger equation will be our starting point on this chapter, and we will examine how it breaks down for many body system. We will observe how some of the best scientists approach this issue utilizing different theorems to get at the contemporary density functional theory. We shall later observe its use in various sectors. In chapter four, we will demonstrate the estimation of electronic and optical properties of our material. We will know the procedure of calculation, and the result of our work. And finally, in chapter five, we will summarize our work and see how we can use our material in various scopes, like energy consumption.

<div align="right">

Chapter 2

</div>

Electronic and Optical Properties

2.1 Overview

The electronic properties of a material are related to the manner in which electrons behave within it. These properties can greatly impact the material's physical and chemical characteristics. This characteristics of a material are influenced by the interactions between electrons and atomic nuclei within that material. Materials possess several crucial electronic properties such as electrical conductivity, resistivity et cetera. This electronic properties of a compound are intricately linked to its electronic band structure, density of states, and other related factors. The optical properties of substances pertain to how they behave when they come into contact with light. Properties such as absorption, reflection, and refraction, among others, can be noticed. In this section, we will be discussing some optical properties. This chapter will cover topics such as band structure, density of states, and various optical properties.

2.2 Band-Structure

The arrangement of energy levels or bands that are occupied by electrons in a material is referred to as band-structure. These bands develop as a result of the periodic potential that the electrons in a crystalline material encounter. When atoms combine to create a crystal, their energy levels divide into discrete levels with small spacings. The permitted energy levels in a solid create bands of states that are isolated from one another by spaces where there are no energy states. The energy scale where no electron state can remain is referred as the band-gap. Other names for it are "Energy gap" and "Fobiddrn gap". The energy difference between the top of the valance band (VB) and the bottom of the conduction band (CB) is another way to describe it [34].

The VB is occupied with the valance electrons from an atom. These valence electrons have no effect on conductivity. The conduction band is either empty or occupied with electrons that have leapt from the valance band. The energy level of it is higher than the valance band. The conductivity of a metal is influenced by the electrons which are situated on conduction band. If we denote band-gap energy in momentum space with $E_g(k)$, then

The conduction band energy:

$$E_c(k) = E_g(k) + \frac{\hbar^2 k^2}{2m_e} \tag{2.1}$$

The valance band energy:

$$E_v(k) = -\frac{\hbar^2 k^2}{2m_h} \tag{2.2}$$

Here k, $\hbar$, m_e, m_h represent the wave vector, reduced planck constant, effective mass of electron and effective mass of hole respectively. Figure 2.1 displays the arrangement of VB and CV in the energy band-gap diagram. There must be sufficient energy for an electron to move from VB to CB. The electron becomes free to move inside the crystal once it has crossed the band-gap. In the crystal, this
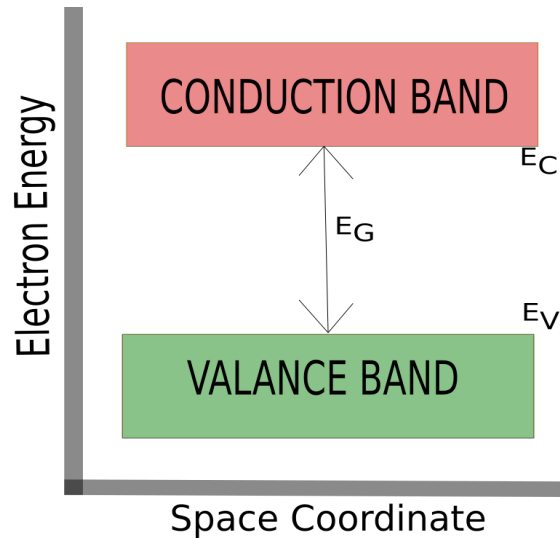
Figure 2.1: Energy band-gap diagram

electron will act as a charge carrier. The bigger the band-gap, the more energy an electron needs to move in CV and operate as charge carrier. Therefore, both the electrical conductivity and the resistivity of a compound are greatly influenced by the band-gap.

2.2.1 Conductor, Insulator, Semiconductor

Based on the differences in band-gaps, the material can be divided into three types: conductor, semiconductor, and insulator.

The term "conductor" refers to a material that has no band-gap at all. So in conductor the VB and CV are being overlapped. As a result, the valance electrons can shift freely in the crystal lattice. Thermal excitation to the conductor metal will increase the vibration and collision of electrons. So the conductivity will decrease and resistivity will increase if we heat a conductor material. Iron, graphite, water, and human body are good examples of conductors.

Large band-gaps with more than 3 eV are a characteristic of insulator. So the VB and CB are separated with huge amount of energy. Thermal stimulation of the insulator causes it to become more conductive and less resistive. Insulators include plastic, rubber, dry air, and glass.

A semiconductor's band-gap, on the other hand, is quite narrow. It is approximately from 0.1 eV to 3 eV. However, there a a few semiconductor materials that have large

band-gap than this range. The band-gap of semiconductor is between conductor and insulator. This property gives them conductivity between conductor and insulator [35]. So unlike insulator, there need a little thermal or other excitation to increase the conductivity of semiconductor. Doping a semiconductor material can also change the conductivity. Semiconductor materials include silicon, germanium, indium, and gallium.

In figure 2.2, we show a diagram showing how the valance band and conduction band are distributed in an insulator, semiconductor, and conductor.
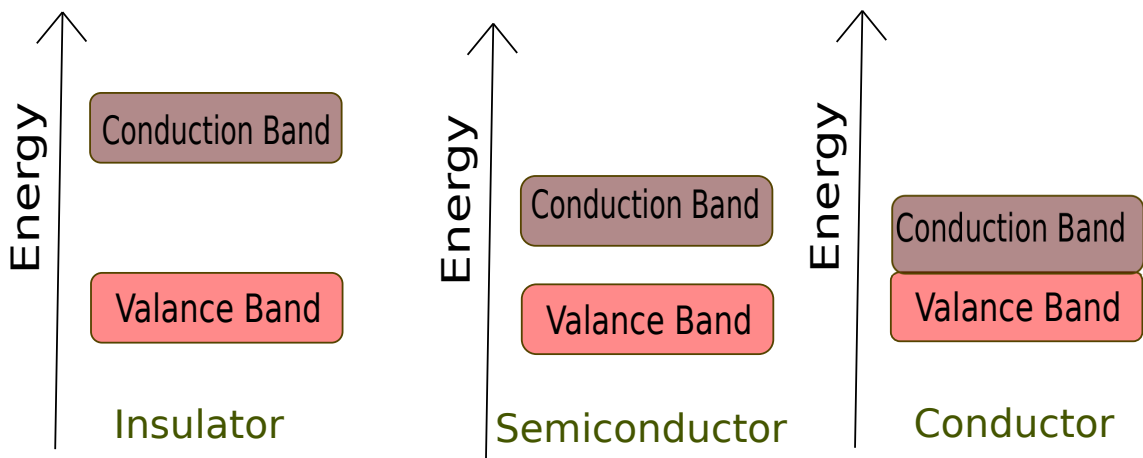
Figure 2.2: Energy band-gap diagram for insulator, semiconductor and conductor

2.2.2   Direct and Indirect Band-Gap

According to the location of top of the VB and the bottom of the CV, the band-gap can be further divided into two parts: direct band-gap, indirect band-gap. For the first case, band-gap, the highest point of the VB and lower point of the CV are situated in identical momentum space. The transition process in direct band-gap materials conserves both energy and momentum. There will be photon-assisted transitions, and that kind of transition is essentially vertical in the energy/wave-vector diagram. The recombination process can be triggered by a little change in momentum. Amorphous silicon and various III-V materials, such as indium arsenite and gallium arsenide, are examples of direct band-gap materials.

The highest point of the VB and lower point of the CV are located in distinct mo-

mentum spaces in indirect band-gap. Since the wave vector must be altered for the transition, the momentum is not conserved in an indirect band-gap, but the energy is. Hence, a photon-associated transition in an indirect band-gap must be accompanied by the emission or absorption of a phonon. There will be phonon-assisted transitions, and that kind of transition is essentially horizontal in the energy/wave-vector diagram. There must be a significant change in momentum for the recombination process to take place. Samples of indirect band-gap compounds include crystalline silicon, germanium, some III-V materials like aluminum antimonide, et ceteraetera.

A diagram for direct and indirect band-gap gaps is displayed on figure 2.3:
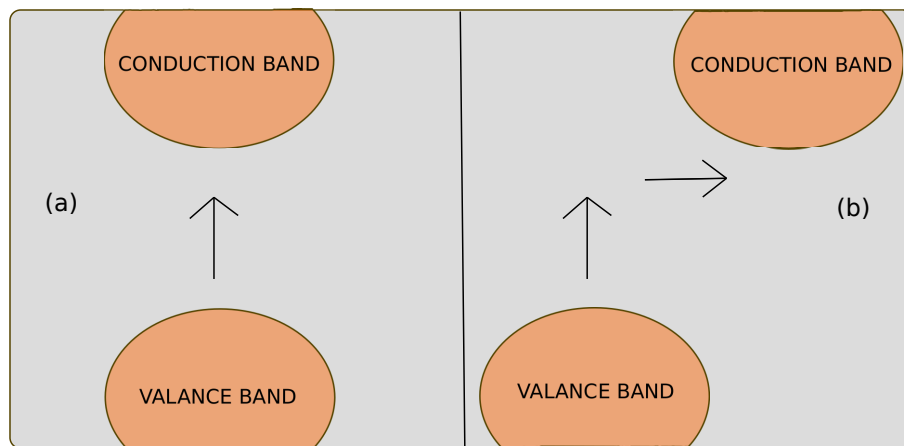
Figure 2.3: (a) Direct and (b) indirect band-gap diagram

2.2.3 Applications

Understanding a compound's band-band-gap is crucial in the evaluation for its prospective applications. As we already know both the electrical conductivity and the resistivity of a compound are greatly influenced by the band-gap. Semiconductor compound's band-gap is a critical factor for figuring out how well they can absorb as well as emit light, also the range of wavelengths in which they can operate. LEDs and laser diodes both emit photons that have energy levels that are similar to the band-gap of a semiconductor they are constructed from. Increasing the band-gap of an LED or LASER will result in a change of color. In both cases, the color of light can be shifted by increasing its energy [36]. Photovoltaic cells can be made from

various materials, and the band-gap of each material differs. For electricity to be generated, a photovoltaic cell requires a photon to hit it with an energy that exceeds the band-gap of compound it's made of. In addition, it is beneficial to construct other renewable energy devices for high power applications, such as transducers, and so on.

2.3 Density of States

A significant notion in the electrical structure of materials is the density of states (DOS). It details the variety of electronic states that can exist in a material at different energy levels. DOS specifically indicates the quantity of electrons on a given energy range per unit volume of the substance. It can be written as for the nth band like [37]:

$$D(E) = \int [d\vec{K}] \delta(E - E_{nk}) \tag{2.3}$$

Here, $D(E)$ denotes the DOS at energy E. And:

$$\int [d\vec{K}] = \frac{2}{(2\pi)^n} \int dK \tag{2.4}$$

Say, for 1D, the DOS will be:

$$
\begin{aligned}
D(E) &= \int [d\vec{K}] \delta(E - E_k) \\
&= \frac{2}{(2\pi)} \int dK \delta(E - E_k) \\
&= \frac{2}{\pi} \int \frac{dE_K}{|\frac{dE_K}{dK}|} \delta(E - E_k) \\
&= \frac{2}{\pi} \frac{1}{|\frac{dE_K}{dK}|}
\end{aligned}
\tag{2.5}
$$

We can calculate the DOS for 2D and 3D using this formula.

Knowing the DOS of a structure us in many ways. In condensed matter physics, electrons are confined to a crystal lattice and their energy levels form bands. Energy bands are a fundamental concept that help to explain the electronic properties of materials. The more information about energy band is given in section 2.2. The

density of states allows us to examine how electrons are distributed across various bands. It is an important tools which is used by scientist to understand how electrons perform in substance like metals, semiconductors, insulators. More specifically, electrical conductivity of a material is ascertained from the DOS at Fermi level, which refers the maximum occupied energy level at absolute zero temperature [38]. Due to their high DOS at the Fermi level, metals are excellent conductors of electricity as they have huge number of free electrons available. Semi-conductor has low DOS around the Fermi level. As a matter of tiny band-gap in semiconductors, DOS rises sharply as the energy level near the lowest point of CV and falls as the energy level approaches the highest point of VB. Comparing with this two, insulator has wide band-gap with low DOS close to Fermi level, that hinders electron movement and leads to high resistivity.

The DOS can be used to understand how a material interacts with light in the context of its optical properties. When light contacts with a substance, it can excite electrons above the Fermi level, moving them from occupied to unoccupied states. The likelihood of this excitation is influenced by both the energy divergence in the midst of the initial and last states and the DOS at the incident photon energy. For instance, there will be a large number of states accessible for the electrons to be stimulated into if a material has a high DOS at the energy of the incident photons. Since more light at that energy will be absorbed by the substance, the absorption will be stronger. A substance will absorb less light and look transparent at that energy if the DOS is low because there are fewer possible states. This diagram in figure 2.4 aims to compare the density of states in three different materials: a metal, semi-metal, along with semiconductor or insulator. In each case, E_f denotes the Fermi level. In conclusion, energy bands and DOS are ideas that are connected and that shed light on the electrical characteristics of materials. The behavior of electrons in substance for a various applications can be predicted and controlled by scientists and engineers by understanding how the DOS varies with energy within various energy bands.
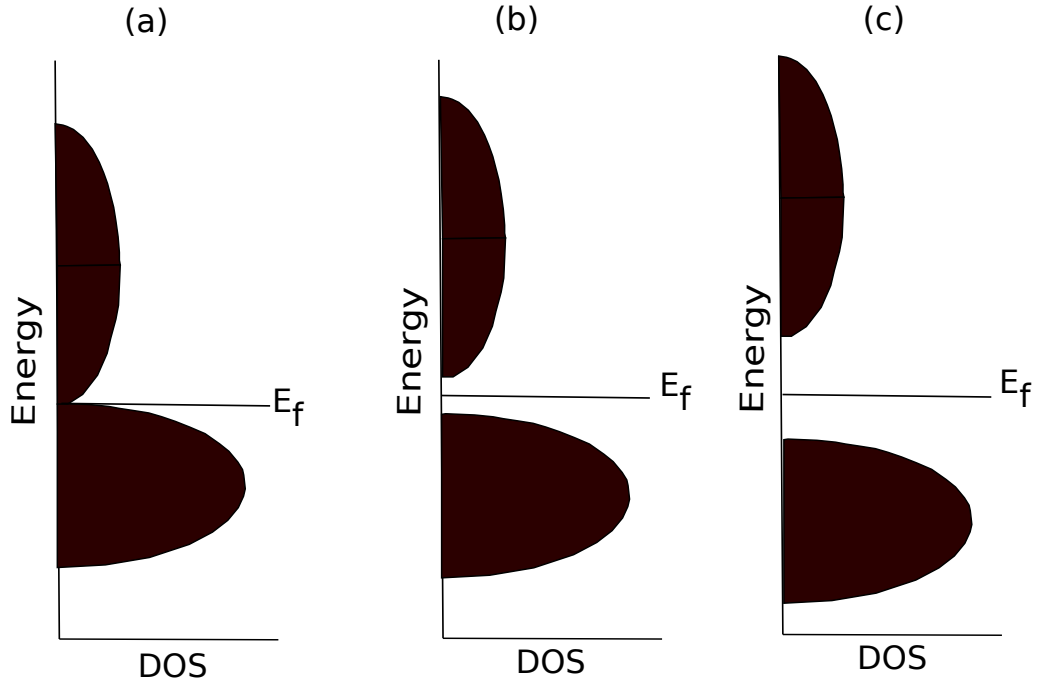
Figure 2.4: A DOS diagram of (a) conductor, (b) semiconductor, along with (c) insulator

2.3.1 Partial Density of States

From section 2.4 we know that the DOS stands for the quantity of electronic states per unit energy. It's useful for identifying the material's electrical and optical characteristics. But it never reveal the distribution of electronic states among the material's atoms and orbitals. Partial density of states (PDOS) enters the picture in this situation.

PDOS examine how different atoms or orbitals contribute to the overall DOS. By dividing the overall DOS into contributions from specific atoms and atomic orbitals, it gives a additional thorough description of a material's electronic structure.

Let's think of a compound made of two different atom types, for instance. The two types of atoms' effects to the total DOS can be distinguished using the PDOS analysis. The relationship between the proportionate amounts of each type of atom and the compound's electronic characteristics may then be understood using this knowledge. In parallel, it can be used to examine how various orbitals affect a material's electrical characteristics. This property is really beneficial in various ways. Like, in a semiconductor, we can use PDOS to study the valence and conduction bands separately. By doing this, we can identify which states are responsible for absorbing

and emitting light. This information is useful for designing semiconductors with specific properties and applications.

2.4 Optical Properties

2.4.1 Complex Dielectric Function

The complex dielectric function is a complex quantity that characterizes how a material reacts to an electromagnetic field that is applied to it. It is commonly represented by the symbol ϵ and referred to as the complex relative permittivity.It is possible to determine all optical properties of materials from it. The dielectric function is dependent on frequency of electron gas and can be written as $\epsilon(w)$. It has two parts real and imaginary and they can be expressed with the relation [39]:

$$\epsilon(w) = \epsilon_1(w) + i\epsilon_2(w) \tag{2.6}$$

Here $\epsilon_1(w)$ and $\epsilon_2(w)$ represent real and imaginary part respectively. The real part describes the ability of the material to store energy in an electromagnetic field, while the imaginary part describes the loss of energy due to absorption or scattering by the material. The formula for calculating $\epsilon_2(w)$ with cubic symmetry substance [40]:

$$\epsilon_2(w) = \frac{8}{2\pi w^2} \Sigma_{nn'} \int_{BZ} |P_{nn'}(k)|^2 \frac{dS_k}{\nabla w_{nn'}(k)} \tag{2.7}$$

And $\epsilon_1(w)$ can be found using Kramers–Kronig relation which is [41, 42]:

$$\epsilon_1(w) = 1 + \frac{2}{\pi} P \int_0^\infty \frac{w'\epsilon_2(w')}{w'^2 - w^2} dw' \tag{2.8}$$

In equation 2.7, $w_{nn'}$ is the energy difference between the two states, dS_k is an energy surface with constant value, and $P_{nn'}$ s the dipole matrix element between the initial and final states and in equation 2.8. In 2.8, P denotes the principal part of the integral. The dielectric function is a useful tool for calculating various optical properties, as we will explore in the following sections.

2.4.2 Absorption Coefficient

The absorption coefficient quantifies the degree to which a substance absorbs electromagnetic radiation, including light. The "absorption coefficient" is the percentage of radiation absorption per unit distance through a material to the amount of radiation that hits the material. The absorption coefficient depends on a number of things, like material's composition, structure, thickness, along with frequency or wavelength of the radiation that hits it. Generally, materials that are more thick or have electrons that are more tightly bound are likely to absorb radiation more effectively than materials that are less thick or have electrons that are more spread out.

Mathematically, the absorption coefficient which is generally denoted as α can be defined simply from Beer–Lambert's law formula [43]:

$$\alpha = \frac{1}{l} ln(\frac{P_O}{P}) = \frac{2kw}{c} = \frac{2.303A}{l} \tag{2.9}$$

Here P_O, P, l, A represents incident intensity, transmitted intensity, distance traveled through the medium (in cm) and absorbance respectively. The absorption coefficient is greatly influenced by the band-gap of the substance. Equation 2.10 shows the dependency of α with band-gap energy E_g [44].

$$\alpha = K \frac{(h\vartheta - E_g)^n}{h\vartheta} \tag{2.10}$$

Here, K is a constant. The value of n varies depending on the kind of the transition. The absorption coefficient can be represented by the dielectric constant using the equation 2.11 [45].

$$\alpha(w) = \frac{\sqrt{2}w}{c} \big[\big\{ \epsilon_1(w)^2 + \epsilon_2(w)^2 \big\}^{\frac{1}{2}} - \epsilon(w)^2 \big]^{\frac{1}{2}} \tag{2.11}$$

The absorption coefficient holds significant importance in various fields, including spectroscopy, imaging, and optoelectronics. Measuring the absorption coefficient at various wavelengths can offer valuable insights into the electronic and atomic

structure of compound. Additionally, it's crucial to control absorption coefficient by selecting appropriate materials and designing devices to achieve high efficiency for the prosperity of optical equipment, photodetectors, and solar cell.

2.4.3 Refractive Index

The term used to describe the extent to which the speed of light is reduced when it travels through a material is known as the refractive index. The definition of the term is the ratio of speed of light at a given substance to its speed in vacuum. A straightforward mathematical formula can be used to express the refractive index, which is typically denoted by the symbol μ is:

$$\mu = \frac{V_o}{V} \tag{2.12}$$

Here, V represents speed of light in substance and V_o represents speed of light in space $(3 \times 10^8 ms^{-1})$. The relationship between the refractive index $n(w)$ as a function of frequency and the dielectric constant can be expressed through equation 2.13, as stated in reference [45].

$$n(w) = \frac{\sqrt{\left[\left\{\epsilon_1^2 + \epsilon_2^2\right\}^{\frac{1}{2}} + \epsilon_1(w)^2\right]}}{\sqrt{2}} \tag{2.13}$$

Refractive index controls both the amount of light bending (or refraction) that occurs when light travels through a material and the angle at which light is reflected to its outermost layer. A substance's refractive index is influenced by its chemical make-up, crystal structure, and additional elements like pressure and temperature. There is another parameter known as complex refractive index which is also a parameter that characterizes the way in which light is bent when it traverses a substance. As we know, the refractive index typically refers to a real number that is determined solely by the characteristics of the material. However, the complex refractive index is a more comprehensive value that consists of both a real and imaginary component.

The complex refractive index can be expressed by the formula [46]:

$$\bar{C} = A(w) + iB(w) = \epsilon^{\frac{1}{2}} \tag{2.14}$$

Here, C, A, B, ϵ represent to complex refractive index, real part, imaginary part, dielectric function respectively. The real and imaginary can be determined by the formula:

$$A = \frac{1}{2}[\epsilon_1(w)^2 + \epsilon_2(w)^2 + \epsilon_1(w)]^{\frac{1}{2}} \tag{2.15}$$

$$B = \frac{1}{2}[\epsilon_1(w)^2 + \epsilon_2(w)^2 - \epsilon_1(w)]^{\frac{1}{2}} \tag{2.16}$$

The refractive index is essential to the creation optical equipment, including lenses, prisms, and fibre optics. Manipulating the path of light, creating images, focusing or dispersing light, and transmitting it over a wide area with minimal loss is possible with the governing of refractive index for various materials. The refractive index plays an essential part in determining colour of materials since it influences the collaboration of light with them.

2.4.4 Optical Reflectivity

The percentage of incident light that is reflected from a material's surface is referred to as optical reflectivity. It is described as the proportion of reflected radiation intensity to incident radiation intensity. It can be measured by the formula [46]:

$$D(w) = \left|\frac{\bar{C} - 1}{\bar{C} + 1}\right| \tag{2.17}$$

Here, D, C represent reflectivity and complex refractive index respectively. The equation 2.18 shows how the optical reflectivity can be directly represented by the dielectric constant, as stated in reference [45].

$$R(w) = \left|\frac{\sqrt{\epsilon_1(w) + i\epsilon_2(w)} - 1}{\sqrt{\epsilon_1(w) + i\epsilon_2(w)} - 1}\right|^2 \tag{2.18}$$

The optical reflectivity is influenced by various factors like material's composition,

structure, and surface properties. Additionally, wavelength as well as angle of the incident radiation also play a significant role. Materials that have smooth and shiny surfaces generally have higher reflectivity compared to those with difficult or textured surfaces. Optical reflectivity finds its applications in various fields like mirror, and also the development of materials for use in photovoltaics, sensing, and nano-photonics. It is affordable to alter the motion and movement of light, improve light-matter encounters, and develop fresh optical effects by governing the reflectivity of various materials.

Chapter 3

Density Functional Theory

3.1 Overview

Computational methods have now become an essential aspect of the scientific world, particularly in the calculation of issues. Computers and numerical approaches are crucial for issues involving enormous quantities of particles, data, and so on that cannot be solved analytically. Furthermore, it necessitates a large amount of resources or financial support for the experiment.

DFT is a type of ab initio method that is often referred to as a computational quantum mechanical modeling method. The method is well-known at the matter of quantum chemistry, condensed matter physics, materials science et cetera. The application of this method starts with remedying the many-body Schrödinger equation problem. However, DFT is more than just another method to solve the Schrödinger equation. DFT provides an entirely distinct approach to any interacting problem, translating it perfectly to more simple non-interacting problem. This methodology is broadly utilized for resolving a variety of issues, with the electronic structure problem being the most common [47]. In DFT, the electron density is used as the fundamental factor, instead of the wave-function. Another method for solving the many-body Schrödinger equation is the Hartree-Fock approach, that uses

wave-functions to describe the electronic figure of atoms and substance. However, this methods has several drawbacks, including a high cost of calculation time for investigating big systems. But DFT has demonstrated superior accuracy at a reduced computing cost, making it superior to all other approaches. This facts makes DFT the most useful method to analyze electronic structure. Walter Kohn with his co-workers developed this "Density functional theory" and find out the way of using the electron density to resolve the Schrödinger equation. For his timeworn work, he got novel prize in 1998 [48]. The chapter describes their work in broad strokes, beginning with fundamental quantum physics, its issues, and how DFT resolves them.

3.2   The Schrödinger Equation

In 1925, Erwin Schrödinger postulated the Schrödinger equation that governs the wave-function of quantum mechanical system, that was published the later year of 1926 [49]. The simple form of the non-relativistic Schrödinger equation:

$$H\psi = E\psi \tag{3.1}$$

Here, H is the Hamiltonian operator, ψ is the eigen-function or wave-function, and E is the Energy eigen-value. The Hamiltonian contains the information of kinetic (T) and potential (V) energy for all particles of the system. For a single particle, it is expressed by the following equation:

$$H = T + V = \frac{P^2}{2M} + V \tag{3.2}$$

Here P is the momentum operator which can be expressed as:

$$P = -i\hbar\nabla \tag{3.3}$$

In 3-D cartesian form, the ∇ is:

$$\nabla = \frac{\partial}{\partial x} + \frac{\partial}{\partial y} + \frac{\partial}{\partial z} \tag{3.4}$$

So for a single particle, the time-independent Schrödinger equation become:

$$E\psi = -\frac{\hbar^2}{2M}\nabla^2\psi + V\psi \tag{3.5}$$

And using the Energy operator as:

$$E = i\hbar\frac{\partial}{\partial T} \tag{3.6}$$

The time-dependent Schrödinger equation becomes:

$$i\hbar\frac{\partial}{\partial T}\psi = -\frac{\hbar^2}{2M}\nabla^2\psi + V\psi \tag{3.7}$$

There are several well-known examples, such as a particle in a box or a simple harmonic oscillator, in which the Hamiltonian can be expressed in a straightforward manner, and the Schrodinger equation can be handled precisely. However, system with large number of molecule is complicated. For example, a Hamiltonian operator for a system consisting of consisting of N_i number of atoms of species i with atomic number Z_i [50]:

$$H = -\frac{\hbar^2}{2}\sum_i \frac{\nabla^2_{\vec{R_i}}}{M_i} - \frac{\hbar^2}{2}\sum_i \frac{\nabla^2_{\vec{r_i}}}{m_e} - \frac{1}{4\pi\epsilon_0}\sum_{i,j}\frac{e^2 Z_i}{|\vec{R_i} - \vec{r_j}|} + \frac{1}{8\pi\epsilon_0}\sum_{i\neq j}\frac{e^2}{|\vec{r_i} - \vec{r_j}|} + \frac{1}{8\pi\epsilon_0}\sum_{i\neq j}\frac{e^2 Z_i Z_j}{|\vec{R_i} - \vec{R_j}|} \tag{3.8}$$

In this equation R_i and M_i are the position and mass of nuclei i respectively, and r_i and m_e are position and mass of electron i respectively. The first two terms of the right hand side describe the kinetic energy of nuclei and electrons. The next three terms describe the potential energy of the system. This potential energy arising from the attraction between electron-nucleus, electron-electron, nucleus-nucleus interaction. It is quite a mass to try to find a solution for this kind of system, as we need to consider every single particle interaction in the system. As Paul Dirac [51] once told that we fully understand the basic physical laws that make up a huge section of physics. But hardest part is using these rules correctly to solve complicated equations that be solved quickly. Even if the rules that govern the problem are easy

to understand, it is very hard to figure out how to turn them into solutions that work.

For one particle or electron, a perfect analytical approach is feasible. One possible way of solving the many-body issue could be a numerical solution. The numerical solution is possible, but the problem is with a large number of variables, which is 3N for the N number of particles involved in the wave-function ψ. As Hartree said [52], there can be a huge amount of data needed to fully describe a system with many factors. In fact, there are 78 different factors that need to be set for just one wave-function of neutral Iron. Even if we only looked at ten values, we would still need more than 10^{78} entries, and that's assuming that symmetry could cut this number down in some way. Simply put, there aren't sufficient atoms through the solar system to make enough paper for a table like this. So, it's clear that advanced math skills are needed to deal with these kinds of complicated processes. Also,there are trouble with interpretation. As Feynman said [52], not only is it hard to solve the equations in quantum physics, but it's also hard to understand what the answer means. So, the major problem in quantum mechanical system of many particles like electron can be summarize as follow:

- Large number of variables.

- Lack of easy interpretation.

- The electron-electron correlations.

3.3   The Wave-Function

The word wave-function (ψ) was used several times in the previous section. As a result, and in order to better understand what follows, a deeper inspection of the wave-function is taken. Below, we will see different characteristics of the wave-function:

- The wave-function ψ, which contains all the information about the particle's

state, is a function of $\psi = \psi(\vec{r}, t)$. For N particles, the wave-function is simply:

$$\psi = \psi(\vec{r_1}, \vec{r_2}, \vec{r_3}, ..., \vec{r_N}, t) \tag{3.9}$$

It is a single value, generally complex function and finite everywhere.

- Basically, $\psi(\vec{r}, t)$ is the probability amplitude of finding a particle in position $\vec{r}$ and time t. If $\psi = \psi(\vec{r}, t)$ is large at any point, the probability of finding the particle in there is large and vice-versa.

- The square of wave-function is the probability of finding a particle in position $\vec{r}$ and time t [53]. Mathematically, it can be present like:

$$|\psi(\vec{r}, t)|^2 = \psi^* \psi \tag{3.10}$$

The square of wave-function is also known as probability density.

- For N particles where the wave-function is the function of $\psi(\vec{r_1}, .., \vec{r_N}, t)$ even if we change the positions of two particles, the probability density will remain unchanged. So:

$$|\psi(\vec{r_1}, \vec{r_2}, .., \vec{r_i}, \vec{r_j}..., \vec{r_N}, t)|^2 = |\psi(\vec{r_1}, \vec{r_2}, .., \vec{r_j}, \vec{r_i}..., \vec{r_N}, t)|^2 \tag{3.11}$$

What happens there is that during a particle exchange, the wave-function only behave in one of two ways. The first is a symmetrical wave-function. In this case, the particles exchange does not alter as a result of the exchange. This is equivalent to bosons. They are the particles with an integer or zero spin. The alternative possibility is an anti-symmetrical wave-function. In this case, when the particles exchange, they change the sign. This is equivalent to fermions. They are the particles with half-integer spin [54,55]. Only electrons, which are classified as fermions, are of interest in the current work. The anti-symmetric fermion wave-function is what leads to the Pauli principle, which asserts that no two electrons can occupy the same state at the same time and when we talk about "state", we are referring to the orbital and spin components of the

wave-function [56].

For simplicity, we will use time-independent wave-function from now on.

- The probability of finding particles in a volume element is:

$$|\psi(\vec{r_1}, \vec{r_2}, \vec{r_3}, ..., \vec{r_N})|^2 d\vec{r_1} d\vec{r_2} d\vec{r_3}....d\vec{r_N} \qquad (3.12)$$

As all particles must be found somewhere in space,the normalization condition of the wave-function gives us:

$$\int d\vec{r_1} \int d\vec{r_2} \int d\vec{r_3}..... \int d\vec{r_N} |\psi(\vec{r_1}, \vec{r_2}, \vec{r_3}, ..., \vec{r_N})|^2 = 1 \qquad (3.13)$$

So the wave-function is square-integral and continuous everywhere [57].

- The expectation value of the appropriate observable for a wave-function can be obtained by first calculating the expectation values of the operators associated with that wave-function [58]. So, for an operator $A(\vec{r_1}, \vec{r_2}, \vec{r_3}, ..., \vec{r_N})$, we can express it as:

$$\hat{A} = \langle A \rangle = \int d\vec{r_1} \int d\vec{r_2} \int d\vec{r_3}..... \int d\vec{r_N} \psi^*(\vec{r_1}, \vec{r_2}, \vec{r_3}, ..., \vec{r_N})$$
$$A(\vec{r_1}, \vec{r_2}, \vec{r_3}, ..., \vec{r_N}) \psi(\vec{r_1}, \vec{r_2}, \vec{r_3}, ..., \vec{r_N}) \qquad (3.14)$$

3.4 Born-Oppenheimer Approximation

The simple form of time-independent Schrödinger equation having "e" electrons and "n" nuclei is:

$$E\psi(\vec{r}_1, \vec{r}_2, ..., \vec{r}_e, \vec{R}_1, \vec{R}_2, ..., \vec{R}_n) = H\psi(\vec{r}_1, \vec{r}_2, ..., \vec{r}_e, \vec{R}_1, \vec{R}_2, ..., \vec{R}_n) \qquad (3.15)$$

Here, $\vec{r}$ and $\vec{R}$ describe the position of electron and nuclei respectively. The exact form of Hamiltonian is given in equation (3.8). The weight of a nuclei is significantly greater than that of an electron. It is possible to think of the entire nuclear wave-function as an incoherent superposition of individual wave packets. The individual

nuclear wave packets are often highly localised since the nuclear masses are normally large enough. Where they move, potential has a sufficiently large arc of curvature. Atomic nuclei can therefore be regarded as classical particles [59]. So, it needs more energy for nucleus to move with respect to electron. In other words:

1. Based on the standpoint of an electron, the locations of nuclei are considered to be stationary.

2. Based on the standpoint of atomic nuclei, the locations of electrons are updated instantaneously.

On the base of this characteristics, Born and Oppenheimer prefer for the segregation of nuclear motion from electronic motion. On the timeline of electronic transitions, it is possible to state that the base movement can be disregarded, indicating that it has no bearing on these changes [60]. This kind of separation is called Born-Oppenheimer approximation. On this approximation, the position of nuclei is fixed, but position of electron is not. As a result, the kinetic energy term for nuclei in equation (3.8) become zero and nuclear nuclear interaction does not change. So the total Hamiltonian is replaced by electronic Hamiltonian, which is:

$$H_{ele} = -\frac{\hbar^2}{2}\sum_i \frac{\nabla^2_{\vec{r_i}}}{m_e} - \frac{1}{4\pi\epsilon_0}\sum_{i,j}\frac{e^2 Z_i}{|\vec{R_i}-\vec{r_j}|} + \frac{1}{8\pi\epsilon_0}\sum_{i\neq j}\frac{e^2}{|\vec{r_i}-\vec{r_j}|} \qquad (3.16)$$

On the left hand side of the equation, the first, second, third term indicate the kinetic term($\hat{T}$), nucleus-electron attraction($\hat{V}$) and electron-electron repulsion($\hat{U}$) respectively. This equation is simpler than equation (3.8). The sole input required for the($\hat{T}$) and the ($\hat{U}$) is the electron number. However, the nucleus-electron attraction term depends on the system. When there are no external magnetic or electrical fields, the expectation value of $\hat{V}$ is also frequently written as the external potential V_{ext} [58]. So we can say the external potential is the only element of the electronic Hamiltonian that is dependent on the atomic or molecular system. After learning about V_{ext}, we must understand the system's wave-function. However, we can accomplish this for a very small system using our knowledge. Additional approximations must be made to find conclusion for larger systems.

3.5   The Hartree and Hartree-Fock Approximation

The Hartree and Hartree-Fock approximation are methods in quantum mechanics used to approximate the behavior of a many-particle arrangement, like electrons in an atom.

The strategy put forth by Hartree (1928) can be regarded as the initial solution to the many-electron problem. He asserted that we may view the wave-functions of multiple electrons can be derived straightforwardly from one electron orbital. He applies self-consistent field(HSCF) to support his assertion [61]. According to his theory, the system treats each particle as if it were traversing the mean field created by all the rest of the particles, instead of direct interaction between them. In other words, electric field that an electron experiences is caused by both the nucleus's core potential and the field that the other electrons have formed. By assuming a total wave-function in a shape a product of the following, the HSCF equations can be deduced using a variational principle [62](This reference [63] serves as a helpful resource for the basic ideas of principles of variational calculus):

$$\Phi(\vec{r}) = \prod_{i=1}^{N} \phi_i(\vec{r}_i) \tag{3.17}$$

Because it offers a comparatively easy method for estimating the characteristics of huge systems of interacting particles, this approximation is frequently helpful. However, in this approximation, electrons are considered to be distinguishable. But electrons are not distinguishable. They are indistinguishable fermion and follow Pauli exclusion principle. This approximation does not follow the principle of anti-symmetry of the wave-function [64, 65]. Also, it can be erroneous for systems with strong interactions.

By taking into account the fact that particles are indistinguishable fermions or bosons subjected to the Pauli exclusion principle, the Hartree-Fock approximation goes a step further. It also implies that the wave-function used to describe the system's state be either symmetric or antisymmetric.The method takes into consideration these symmetry constraints through generating a single Slater determinant wave-function that characterizes the actions of all the particles in the system. So

the wave-function become [66, 67]:

$$\Phi_{HF}(\vec{r}_1, \vec{r}_2, ..., \vec{r}_N) = \frac{1}{\sqrt{N!}} \begin{vmatrix} \phi_1(1) & \phi_2(1) & \phi_3(1) & \ldots & \phi_N(1) \\ \phi_1(2) & \phi_2(2) & \phi_3(2) & \ldots & \phi_N(2) \\ \ldots\ldots\ldots\ldots\ldots\ldots\ldots\ldots\ldots\ldots\ldots\ldots\ldots \\ \phi_1(N) & \phi_2(N) & \phi_3(N) & \ldots & \phi_N(N) \end{vmatrix} \tag{3.18}$$

$$= SD\{\phi_1(1)\phi_2(2)\phi_3(3)......\phi_N(N)\}$$

Here $\phi_i(j)$ indicates the ith electron's spin orbital, which is made up of both spin and spatial components. Where j denotes the spatial and spin coordinates of electron j, that has been compressed into a variable. The root of N is normalization factor. This formula ensures that wave-function flips its signature as the coordinates of 2 electrons are swapped out. Also, it disappears if two electrons have the same coordinates or if two of the electrons have the same wave-function.

The Hartree and Hartree-Fock approximations ignore any effects of electron correlation by assuming that electrons move independently of one another. Actually, electrons are not autonomous; rather, they engage in Coulombic repulsion and exchange interactions with one another. When these interactions are ignored, predictions of molecular attributes like bond lengths, bond angles, and energy may be inaccurate. The scalability of the Hartree and Hartree-Fock approximations is still another drawback. For larger molecules, these techniques become computationally expensive, making it challenging to forecast the electrical structure of complicated systems. The Hartree-Fock technique also implies an inference that electron wave-function might be adequately characterized by a solo determinant, which may not necessarily be true for multi-reference platforms in which electronic wave-function is considerably influenced by multiple configurations.

3.6 The Electron Density

In previous sections, we observed the challenges involved in solving the Schrödinger equation for larger structures. Scientists needed to come up with an approximation or model for wave-function that will give logical outcome. When establishing such a

model, it's worth to remember that wave-function is not observable directly. Instead, we can measure is the probability that N electrons at some particular set of position $(\vec{r}_1, ..., \vec{r}_N)$. Also, we need to remember that all electrons are identical. So we can not level them as electron 1 or electron N, but we could figure out the probability of any order or set of N electrons being in the coordinates $\vec{r}_1$ to $\vec{r}_N$. Keeping this factors in mind, the electron density which is the fundamental parameter for DFT can be calculated like [68]:

$$n(\vec{r}) = N \sum \int d\vec{x}_2 .... \int d\vec{x}_N \psi^*(x_1, x_2, ..., x_N) \psi(x_1, x_2, ..., x_N) \tag{3.19}$$

The equation relates to the wave-function, which takes into account both spin and spatial coordinates. Specifically, the integral in the equation denotes the probability of detecting an electron with any spin within a given volume element $d\vec{r}_1$. As electrons are identical, multiplying the integral by N gives the probability of discovering any electron in that region. The wave-function $\psi(x_1, x_2, ..., x_N)$ represents the presence of other electrons with random spin and spatial coordinates [68].

By integrating the electron density, we can easily find number of electrons overall.

$$N = \int d\vec{r} n(\vec{r}) \tag{3.20}$$

It renders density a good choice for how quantum physics should be put together. In upcoming sections, we will see how the electron density is a distinctive characteristic of the external potential.

3.7 Thomas-Fermi Theorem

Many people have looked into the subject of explaining the density of a assembly with multiple electrons, which led to the so-called density functional theory. The first exploration has done by Llewellyn Thomas and Enrico Fermi in 1927, which is known as Thomas-Fermi model [69]. The model helps to descrive the electronic structure of many election system. It was made in a semi-classical way soon after the Schrodinger equation was made. It's a semi-classical approach since it borrows some

ideas from quantum mechanics. But the rest of the ideas don't use quantum physics. Instead, they can be operated with regular function. Unlike the wave-function-based approach, this formulation was completely based on electronic density and is seen as a precursor to the modern DFT. The total energy of a system, within the Thomas-Fermi model, is given as a functional of density like $E_{TF}[n(\vec{r})]$. The Thomas-Fermi energy functional composed of three terms, is expressed as follow:

$$E_{TF} = X \int n(\vec{r})^{\frac{5}{3}} d\vec{r} + \int n(\vec{r}) V_{ext}(\vec{r}) d(\vec{r}) + \frac{1}{2} \int \int \frac{n(\vec{r})n(\vec{r'})}{|\vec{r} - \vec{r'}|} d\vec{r} d\vec{r'} \qquad (3.21)$$

The initial phrase is the electronic kinetic energy of a system of electrons in a uniform electron gas that do not interact with each other. We can obtain this by integrating the kinetic energy density of a homogeneous electron gas to $t_0[n(\vec{r})]$ as:

$$T_{TF} = \int t_0[n(\vec{r})] d\vec{r} \qquad (3.22)$$

$t_0[n(\vec{r})]$ is obtained by summing all the free-electron energy states $\epsilon = \frac{P^2}{2M}$ Up to the Fermi wave vector $P_F = [3\pi^2 n(\vec{r})]^{\frac{1}{3}}$ given by:

$$t_0[n(\vec{r})] = \frac{2}{2\pi^2} \int_0^{P_F} \frac{P^2}{2M} N_P dP \qquad (3.23)$$

The term N_P leads to the density of allowed states in reciprocal space given by $\frac{4\pi P^2 V2}{h^3}$. This gives us the result for X as:

$$X = \frac{3}{10} * (3\pi^2)^{\frac{2}{3}} \qquad (3.24)$$

The second term represents the classical electrostatic energy of attraction between nuclei and electron. Here $V_{ext}(\vec{r})$ is the classic coulomb potential arising from the nuclei, given by the following expression:

$$V_{ext}(\vec{r}) = - \sum_{i=1}^{N} \frac{Z_i}{|\vec{r} - \vec{R_i}|} \qquad (3.25)$$

And finally the third term in the energy functional represent the electron-electron interaction of the system. It is approximated by the classical coulomb repulsion

between electrons. This is also known as Hartree energy.

To obtain the ground state density of a system, the Thomas-Fermi equation must be minimized subjected to the constraint that the number of electron is conserved. This type of constraint minimization problem can be solved by using Lagrange multiplayer. Say, the minimization of a functional $A[X]$, subjected to the constraint $B[X]$, leads to the stationary condition:

$$\delta(A[X] - \alpha B[X]) = 0 \tag{3.26}$$

Here α is a constant which is known as Lagrange multiplayer. This minimization leads to the solution of corresponding Euler equation:

$$\frac{\delta A[X]}{\delta X} - \alpha \frac{\delta B[X]}{\delta X} \tag{3.27}$$

Applying this above formula to the Thomas-Fermi model, it will give us the stationary condition:

$$\delta\{E_{TF}[n(\vec{r})] - \alpha(\int n(\vec{r})d\vec{r} - N\} = 0 \tag{3.28}$$

This yields the so-called Thomas-Fermi equation as:

$$\frac{5}{3}Xn(\vec{r})^{\frac{2}{3}} + V_{ext}(\vec{r}) + \int \frac{n(\vec{r'})}{|\vec{r} - \vec{r'}|}d\vec{r'} \tag{3.29}$$

This above equation can be solved using iterative methods to obtain the ground state density. Thomas-Fermi model differs from other models because it is simple, easy to understand, and works for large of temperatures as well as pressures. With this model, we can use density to figure out the estimated term for kinetic energy. In orbital-free DFT, this formula for kinetic energy within Thomas-Fermi theory is also used as a part of better density approximations for kinetic energy. Though Thomas-Fermi theory contains all the necessary ingredients which paved the way to modern DFT, it has many shortcoming as well. And those shortcomings are:

- It tell how atoms will stick together. So, this idea be made up of molecules and solids.

- The estimation of kinetic energy is done in a rudimentary manner. Kinetic energy accounts for a substantial portion of the overall energy. So even small mistakes can add up to big problems.

- Oversimplified descriptions of how electrons interact with each other, which don't take into account many quantum effects.

- The correlation effect is neglected completely.

3.8 Hohenberg-Kohn Theorems

When the Thomas-Fermi approach was first conceptualized, it was thought that the energy could be declared solely by means of its electronic density. It took more than three decades to offer a convincing argument for the validity of this idea, despite the fact that it seemed reasonable at the time. In 1964, Hohenberg and Kohn introduced theorems that established a strong logical basis for the preceding concepts, which they also proved. The idea of DFT is built upon 2 essential theorems provided by Walter Kohn and Pierre Hohenberg. This theorems are known as Hohenberg–Kohn theorems [70, 71]. The theorems with their validity are given below.

3.8.1 Theorem 1

The Hohenberg-Kohn 1st theorem is:

> *The ground state of energy E from Schrödinger equation in a presence of external potential $V(\vec{r})$ is a unique functional of electron density $n(\vec{r})$.*

According to the first theorem, the ground-state density and the external potential correspond one to one. Since the external potential is fixed, the Hamiltonian hence the wave-function ψ is fixed by $n(\vec{r})$. The evidence in support of this theorem is straightforward. Consider the ground states of two N-electron systems that are characterised by 2 external potentials $V_a(\vec{R})$ and $V_b(\vec{R})$. These potentials differ from each other by more than just an additive constant. The corresponding Hamiltonians

with Schrödinger equation are given by:

$$H_a = \hat{T} + \hat{U} + \sum_i V_a(\vec{R}_i) \tag{3.30}$$

$$H_b = \hat{T} + \hat{U} + \sum_i V_b(\vec{R}_i) \tag{3.31}$$

Here, on the the right hand side in both equations, first part is the kinetic energy part which can define as:

$$\hat{T} = -\frac{1}{2} \sum_i \nabla_i^2 \tag{3.32}$$

And the second part is from the electron-electron repulsion. It can define as:

$$\hat{U} = \frac{1}{2} \sum_{i \neq j} \frac{1}{r_{ij}} \tag{3.33}$$

The third part is external potential, which is different in both equations and makes the Hamiltonians different too. The Hamiltonians are corresponds with two different wave-function ψ_a, ψ_b and ground state energy E_a, E_b, where $E_a \neq E_b$.

$$H_a\psi_a = E_a\psi_a; H_b\psi_b = E_b\psi_b \tag{3.34}$$

We assume that two wave-function ψ_a, ψ_b(which is our trial wave-function) yield the same density. Using the variational principle, one can write:

$$E_a = \langle \psi_a|H_a|\psi_a \rangle < \langle \psi_b|H_a|\psi_b \rangle \tag{3.35}$$

Here, the final section is able to be extended as:

$$\begin{aligned}
\langle \psi_b|H_a|\psi_b \rangle &= \langle \psi_b|H_a|\psi_b \rangle + \langle \psi_b|H_a - H_b|\psi_b \rangle \\
&= E_b + \int d^3\vec{r}\, n(\vec{r})[V_a(\vec{r}) - V_b(\vec{r})]
\end{aligned} \tag{3.36}$$

Thus, one has the result:

$$E_a < E_b + \int d^3\vec{r}\, n(\vec{r})[V_a(\vec{r}) - V_b(\vec{r})] \tag{3.37}$$

Interchange the suffixes, 2 and 1, gives the result:

$$E_b < E_a + \int d^3\vec{r}\, n(\vec{r})[V_b(\vec{r}) - V_a(\vec{r})] \tag{3.38}$$

If we sum equation (3.37) and (3.38), the both second term of the right hand side will cancel each other. So, we will get the expression:

$$E_a + E_b < E_b + E_a \tag{3.39}$$

Clearly, this is an impossible expression. Thus, we can say that the energy associated with a specific external potential is a distinct functional of density.

3.8.2   Theorem 2

The 2nd Hohenberg-Kohn theorem is:

> *The electron density that minimizes the energy of the overall functional is the true electronic density, corresponding to the full solution of Schrödinger equation.*

According to the second theorem, it is feasible to ascertain the energy of the ground state based on the number of electrons by utilizing the variational method. By minimizing the system energy with varying electron density at a given external potential, we can reach the ground state energy. In the context of DFT, the principle known as the variational principle is applied, whereby the electron density that results in the lowest system energy is referred to as the ground-state electron density. To prove the statement second theorem, we need to consider the variational principle. The variational principle is useful for obtaining accurate upper bounds to the ground-state energy [72]. To obtain the ground-state energy of a system, one can minimize the energy functional with respect to the trial wave-function. Trial wave-function can be any physically acceptable function that satisfies appropriate boundary conditions. For a many-electron system, the ground-state energy can be expressed as a functional

of the electron density:

$$E[n(\vec{r})] = G[n(\vec{r})] + \int V(\vec{r})n(\vec{r})d\vec{r} \qquad (3.40)$$

The energy functional can be divided into two parts: the first part is the energy of the electrons in the external potential, and the second part is a "universal functional" $G[n(\vec{r})]$ that depends only on the electron density and doesn't depend on V_{ext}. The universal functional is important because it encapsulates all the information about the interactions between the electrons. In other words, if we know the electron density $n(\vec{r})$, we can calculate the value of the universal functional $G[n(\vec{r})]$, and this will tell us everything we need to know about how the electrons interact with each other. In equation, $G[n(\vec{r})]$ can be expressed as:

$$G[n(\vec{r})] = \hat{T} + \hat{U} \qquad (3.41)$$

The true electron density $n_o(\vec{r})$ corresponds to the minimum of this energy functional, that is:

$$E[n_o(\vec{r})] = min\{E[n(\vec{r})]\} \qquad (3.42)$$

Now suppose that we have a trial density $n_p(r)$, which is different from the true density. We can express the total energy as follows:

$$E[n_p(\vec{r})] = G[n_p(\vec{r})] + \int V(\vec{r})n_p(\vec{r})d\vec{r} \qquad (3.43)$$

Since $n_p(r)$ is not the true density, it must have higher energy than the true density. That is:

$$E[n_p(\vec{r})] - E[n_o(\vec{r})] = G[n_p(\vec{r})] - G[n_o(\vec{r})] + \int V(\vec{r})[n_p(\vec{r}) - n_o(\vec{r})]d\vec{r} \qquad (3.44)$$

Since $n_o(r)$ corresponds to the minimum of the energy functional, we have:

$$G[n_p(\vec{r})] - G[n_o(\vec{r})] \geq 0 \qquad (3.45)$$

So,

$$E[n_p(\vec{r})] - E[n_o(\vec{r})] \geq \int V(\vec{r})[n_p(\vec{r}) - n_o(\vec{r})]d\vec{r} \qquad (3.46)$$

This expression shows that for any trial density $n_p(r)$, the difference between its energy and the true ground-state energy is bounded below by the integral of the difference between the trial density and the true density, multiplied by the external potential. The minimum of this difference is achieved only when the trial density matches the true density, that is, $n_p(r) = n_o(r)$. Therefore, we can conclude that the true electronic density corresponds to the comprehensive solution of the Schrodinger equation, which is the electron density that minimises the energy of the overall functional.

The equation (3.40) can be expanded as:

$$E[n] = \int d\vec{r}V_{ext}(\vec{r})n(\vec{r}) + \frac{e^2}{8\pi\epsilon_0}\int d\vec{r}d\vec{r'}\frac{n(\vec{r})n(\vec{r'})}{|\vec{r} - \vec{r'}|} + T[n] + E_{xc}[n] \qquad (3.47)$$

Where:

$$T[n] = \frac{\hbar^2}{2m_e}\int d\vec{r}d\vec{r'}\nabla_{\vec{r}}\nabla_{\vec{r'}}n_1(\vec{r}, \vec{r'})|_{(\vec{r}=\vec{r''})} \qquad (3.48)$$

$$E_{xc}[n] = \frac{\hbar^2}{2m_e}\int d\vec{r}d\vec{r'}\frac{C_2(\vec{r}, \vec{r'})}{|\vec{r} - \vec{r'}|} \qquad (3.49)$$

Here, $n_1(\vec{r}, \vec{r'})$ is one-particle density matrix and $C_2(\vec{r}, \vec{r'})$ is two particle correlation function. And "xc" means exchange-correlation. $E_{xc}[n]$ includes all quantum mechanical effects which are not included in previous terms.

3.8.3 Advantage and Disadvantage

With the help of these theorems, it is possible to calculate all the ground and excited states of many-body wave-functions. Because $n(\vec{r})$ has a single effect on external potential, it also has a single effect on the ground state wave-function, which could be found from computing the full Schrodinger equation for many bodies. It also implies, density of the ground particles entirely and exclusively influences all system attributes. The Hamiltonian resembles the electronic Hamilton operator described

in the formula (3.16), which was the subject of Hohenberg and Kohn's initial investigation because it involved an electron gas. The advantage of Hohenberg–Kohn theorems is that it make the process of resolving the Schrödinger equation simpler by shifting the focus from finding a function of 3N variables (the wave-function) to a function of three variables (the electron density). The Hohenberg-Kohn theorem utilizes the variational principle to establish the connections between potential and density.

Unfortunately, Hohenberg and Kohn's framework is precise, yet it is not very useful in practical calculations. Hohenberg and Kohn together could not offer any way to find the proper electronic density [73]. As there is no explicit formula linking the kinetic energy to the electronic density at this point, determining it accurately is the main challenge. The Laplacian of the one-body density matrix, which is not directly related to the density itself, must be known in order to calculate the kinetic energy term precisely. Because of this, it is challenging to calculate the kinetic energy precisely. The Hohenberg-Kohn theorems are limited in their applicability to ground-state systems exclusively. This means that it cannot be used to describe excited states or dynamics of a system. Another limitation is that the theorem assumes a non-degenerate ground state, which may not always be the case for certain systems.

3.9 Kohn-Sham Formulation

Kohn and Sham proposed a method to solve the problems that arise is the Hohenberg-Kohn theorem [74] based on two approximations described as follows [75]:

1. The ground state density can be understood as the ground state of a system consisting of non-interacting particles in an auxiliary framework.

2. The Hamiltonian of the auxiliary system is formulated using the conventional kinetic energy operator, while the auxiliary potential is regarded as an effective local potential.

Density Functional Theory

The Kohn-Sham theorem postulates that the electron density of the ground state in an interacting system is equivalent to the electron density of the ground-state in a non-interacting system, provided that an effective potential V_{eff} is employed. We disregard all forms of interaction between atoms, electrons, and nuclei in a system that doesn't interact. This approximation best works for densities which are smooth and vary slowly [74]. Kohn and Sham considered a many-body, multi-electronic system composed of non-interacting particles. They solve the system using a modified form of Schrödinger equation for a non-interacting system that produces the same value of ground state electron density as an interacting system. The non-interacting wave-function of a many body wave-function is a Slater-determinant of one-electron wave-function. One can obtain the wave-function by solving this Schrödinger equation (also refers as Kohn-Sham equation):

$$\hat{H}_{ks}\Psi_j = \{-\frac{\hbar^2}{2m_e}\nabla^2 + V_{eff}\}\Psi_j = \epsilon_j\Psi_j \tag{3.50}$$

Here, the term V_{eff} refers to "effective potential", which compensates error due to ignoring interaction. The total energy E ($E = \sum_j \epsilon_j$) is divided into two parts. The known component; which comes from the non-interacting part. And the unknown component; which is also known as exchange-correlation part($E_{xc}[n(\vec{r})]$). It contains all the errors that are contain in a non-interacting system as we neglect all types of interaction between particles. This correlation part can be evaluate using different approximation like "LDA", "GGA" et cetera which will be discussed in section 3.10. The kinetic energy term is divided into two parts; the kinetic energy of non-interacting particles(T_a) and the kinetic energy of interacting particles(T_b). The non-interacting part can be obtain by the equation:

$$T_a[n(\vec{r})] = -\frac{\hbar^2}{2m_e}\sum_i \left\langle\Phi_i|\nabla^2_{\vec{r_i}}|\Phi_i\right\rangle \tag{3.51}$$

The kinetic energy of interacting particles(T_b) can be obtained by approximation methods like "LDA", "GGA" et cetera. Also, the effective potential can be obtained from:

$$V_{eff} = V_{ext} + V_H[n(\vec{r})] + V_{xc}[n(\vec{r})] \tag{3.52}$$

Density Functional Theory

Here, $V_H[n(\vec{r})]$ is Hartree potential, which is obtained by:

$$V_H[n(\vec{r})] = \frac{e^2}{4\pi\epsilon_0} \int d\vec{r'} \frac{n(\vec{r'})}{|\vec{r} - \vec{r'}|} \tag{3.53}$$

And the exchange-correlation potential $V_{xc}[n(\vec{r})]$, is defined as:

$$V_{xc} = \frac{\delta E_{xc}[n]}{\delta n} \tag{3.54}$$

From those considerations, the new Hamiltonian becomes:

$$H = -\frac{\hbar^2}{2m_e} \sum_i \nabla_{\vec{r_i}}^2 + \frac{e^2}{4\pi\epsilon_0} \int d\vec{r'} \frac{n(\vec{r'})}{|\vec{r} - \vec{r'}|} + V_{xc} + V_{ext} \tag{3.55}$$

The major distinction within the formulation and the Hartree formulation is the fact that the Kohn–Sham formulation involves exchange along with correlation in the effective potential. So, Kohn–Sham has about the same amount of work to do as Hartree, but a lot fewer compared to Hartree–Fock. It can be seen that to solve the equation (3.55), we need electron density. To find the electron density requires a single electron wave-function. And to know the wave-function, one must solve the equation (3.55). So to break this circle, the equation is solved in an iterative process as follows:

1. Set a baseline electron density, $n(\vec{r})$, for analysis.

2. Solve the equation using the sample electron density to determine the single particle wave-function $\psi_i(\vec{r})$.

3. Calculate the electron density from the equation below:

$$n_{ks}(\vec{r}) = \sum_i \psi_i^*(\vec{r})\psi_i(\vec{r}) \tag{3.56}$$

4. Examine the calculated electron density $n_k s(vecr)$ to the experimental electron density $n(vecr)$. If the densities are self-consistent, then this is the electron density in the ground-state. Alternately, revise the sample electron density and proceed to step 2.

In the above process, the term "self-consistent" means that the electronic density is changed over and over again until the energy is at its lowest and the electronic Hamiltonian matches the current density. This looping process keeps going until the electronic density converges on an answer that makes sense on its own. The above circle is shown using a flow-chart [76] in figure 3.1.
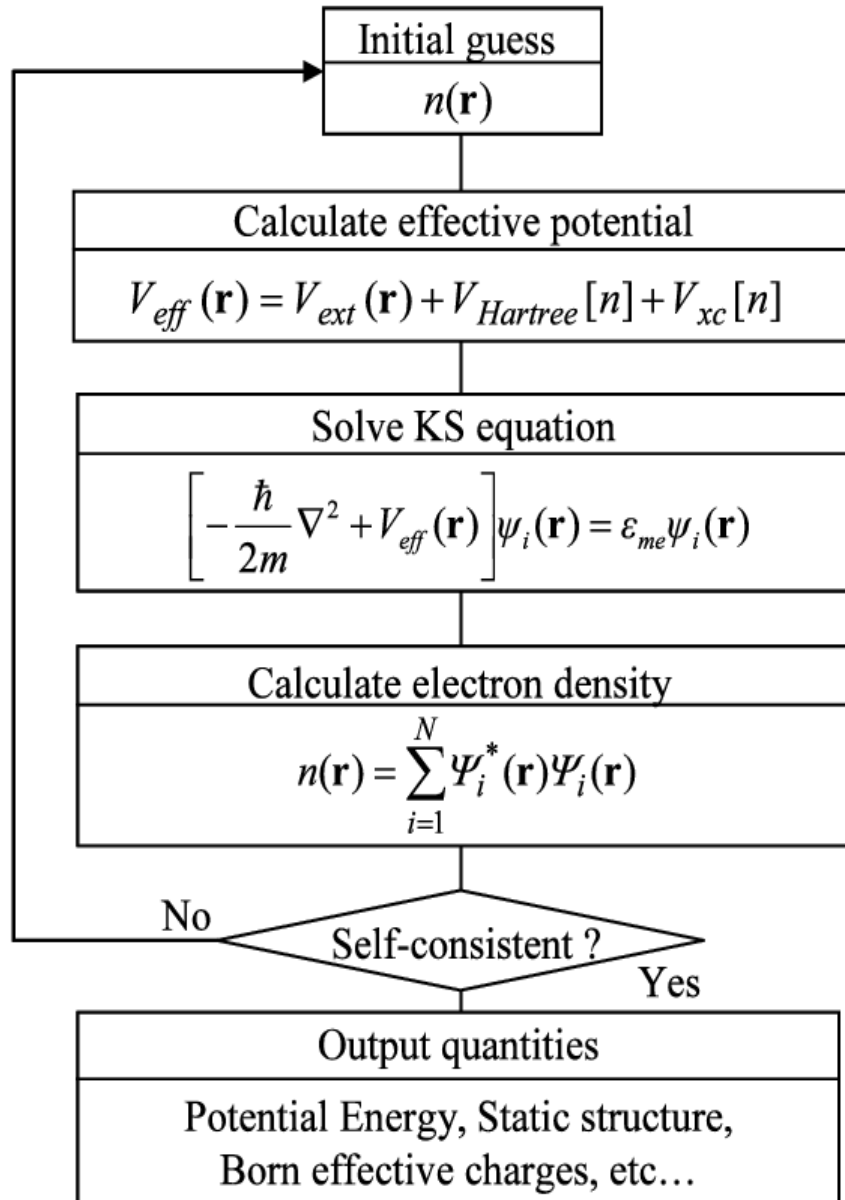
Figure 3.1: Flow chart of solving the Kohn-Sham equation

3.10　Exchange-Correlation Potential

In DFT, the exchange-correlation potential is a word for how the electrons in a material interact with each other. It combines the effects of exchange and correlation, which are two basic ideas in quantum physics that explain how electrons interact with each other. The exchange potential comes from the fact that electrons are identical objects and follow the Pauli exclusion principle, which says that it is

impossible for two fermions that are identical to inhibit the same quantum state simultaneously. The correlation potential comes from the fact that electrons connect with each other through Coulombic forces, which depend on where and how fast they are moving. In DFT, to solve the equation (3.55), we also need an expression for the exchange-correlation potential. For the solution, different theoretical models and estimates are used to get close to the exchange-correlation potential. The accuracy of these rough estimates varies on the type of material being modeled and how it is used. In the next parts, we will talk about and analyze the local density and generalized gradient approximations, which are two of the most common ways to solve the exchange-correlation functional.

3.10.1 LDA

The LDA stands for "local density approximation". Here the exchange-correlation potential is a function of electron density $n(\vec{r})$ only. Walter Kohn described LDA as the forebearer of all approaches in his Nobel lecture [48]. From this approximation, the exchange-correlation energy follows the formula:

$$E_{xc}^{LDA}(n(\vec{r})) = \int n(\vec{r})\epsilon_{xc}(n(\vec{r}))d\vec{r} \qquad (3.57)$$

From spin polarized system [77], the form of the equation is change into:

$$E_{xc}^{LSDA}(n_\uparrow(\vec{r}), n_\downarrow(\vec{r})) = \int n(\vec{r})\epsilon_{xc}(n_\uparrow(\vec{r}), n_\downarrow(\vec{r}))d\vec{r} \qquad (3.58)$$

Here, LSDA means Local Spin Density Approximation. The exchange-correlation energy($\epsilon_{xc}(n(\vec{r}))$) per particle at each point in the system is the same as that of uniform electron gas of same density. The exchange-correlation energy can be divided into two parts; the exchange part and the correlation part. Using the equation 3.54, we can find the exchange-correlation potential as [78]:

$$V_{xc} = \frac{\delta E_{xc}^{LDA}(n(\vec{r}))}{\delta n} = \epsilon_{xc}(n(\vec{r})) + n(\vec{r})\frac{\delta \epsilon_{xc}(n(\vec{r}))}{\delta n} \qquad (3.59)$$

The advantage of LDA is its low complexity, which makes it computationally effective and makes it possible to examine big systems. LDA is the only case where the exchange-correlation functional can be derived exactly. It has been discovered that this approximation is fairly true for a variety of systems, especially for bulk solids. An additional advantage of this approximation is that LDA sheds light on the electrical characteristics of materials, enabling researchers to forecast and comprehend phenomena including chemical reactivity, optical characteristics, and magnetic behavior [79, 80]. This approximation has many disadvantages as well. The solutions of exchange-correlation effects in the LDA are improper when the assumption of an electron gas with a slowly varying density as the starting point is fundamentally false. Examples include the Van der Waals interactions between non-overlapping subsystems, the electronic Wigner crystal, and electronic tails dissipating into space on the surfaces of bounded electronic systems [48]. However, density functional theory may effectively address such issues when using the right approximations.

3.10.2 GGA

GGA stands for "generalized gradient approximation". In this approach, the exchange-correlation potential depends on density($n(\vec{r})$)) as well as the gradient of density($\nabla n(\vec{r})$)) [81]. This approximation is achieved by improving local density approximation [82, 83]. From this approximation, the exchange-correlation energy follows the formula:

$$E_{xc}^{GGA} = E_{xc}^{GGA}[n(\vec{r})), \nabla n(\vec{r})] = \int n(\vec{r}) \epsilon_{xc}(n(\vec{r}), \nabla n(\vec{r})) d\vec{r} \qquad (3.60)$$

By considering the spin components, the equation can rewrite as:

$$E_{xc}^{GGA}[n_\uparrow(\vec{r}), n_\downarrow(\vec{r}), \nabla_\uparrow(\vec{r}), \nabla_\downarrow(\vec{r})] = \int n(\vec{r}) \epsilon_{xc}(n_\uparrow(\vec{r}), n_\downarrow(\vec{r}), \nabla_\uparrow(\vec{r}), \nabla_\downarrow(\vec{r})) d\vec{r} \quad (3.61)$$

GGA is better than LDA at predicting the electronic qualities of materials because it takes both the local electron density and the gradient of that density into account [84, 85]. It also gives a better explanation of how molecules and solids are held together by chemical bonds. It can also predict non-local features like magnetic interactions and exchange-correlation energies. GGA also needs less computer power

than more advanced ways, which makes it easier to use for large-scale calculations. Overall, GGA has made it much easier to simulate and understand how materials behave at the atomic level.GGA corrects too much When the lattice constants of LDA fit better than those of GGA, ionic crystals are the result. But neither LDA nor GGA works well when it comes to transition metal oxides or rare earth elements.

3.10.3 Hybrid Functional

Hybrid functional approximation is a sort of computational method employed in DFT studies. It was created by A. Becke [48]. Hybrid functionals try to get around this problem by mixing parts of both the local density approximation (LDA), and the generalized gradient approximation (GGA). In this method, the first exchange-correlation energy was written in the format:

$$E_{xc}^{hyb} = \gamma E_x^{ks} + (1 - \gamma)E_{xc}^{GGA} \tag{3.62}$$

Here, E_x^{ks} is the exchange energy calculated with the exact Kohn-Sham wave-functions. And γ is known as fitting parameter. Currently, there are numerous popular hybrid functionals available, including B3LYP, PBE0, and HSE06. Each of these functionals has its own unique strengths and weaknesses, which depend on the specific material and property being studied.

The main benefit of hybrid functionals is that they blend the best parts of both LDA and GGA functionals. LDA does a good job of describing how the density changes slowly, but it doesn't account for the exchange-correlation energy in systems where the density changes. GGA, on the other hand, gives a better picture of the exchange-correlation energy, but it often overestimates or underestimates certain properties, such as band-gaps, bond lengths, and reaction energies. Hybrid functionals get around these problems by adding a small amount of exact Hartree-Fock exchange to the normal GGA functional. This makes the predicted properties more accurate, especially for systems with big band-gaps, states that are localized, and atoms of transition metals. The result is a hybrid functional that is a mix of LDA and GGA parts. This gives a good balance between accuracy and cost of processing.

In general, the benefit of hybrid functional approach is better than LDA and GGA functionals because it is more accurate and stable. This quality makes it handy for predicting the properties of materials and molecules in a wide range of applications, such as catalysis, energy storage, and electronic devices.

3.11 Applications

There are several uses of DFT in physics, chemistry as well as materials science. Here are some uses of DFT as follows:

- DFT is a great way to learn about things like electronic properties of materials like band-gap, DOS et cetera. As we already know, The change in energy between a material's VB and CV is called the band-gap. With the aid of Kohn-Sham equations, which describe the behaviour of electrons that don't interact with each other in the presence of an effective potential, DFT calculation is helpful for correctly predicting the band-gap of a substance. DOS, on the other hand, offers details regarding the distribution of electronic states within a material's band structure. By integrating the density of states over the allowable energies, DFT computations can be utilized to determine the DOS.

- DFT can be used to study the X-ray absorption spectra and X-ray emission spectra of material [86]. X-ray absorption spectroscopy (XAS) examines how the amount of X-rays absorbed by a sample changes with the energy of the X-rays. The absorption spectrum shows how the particles in the material are put together electronically. On the other hand, X-ray emission spectroscopy (XES) tracks how the energy of the light that a sample gives off after being excited by X-rays. DFT can be used to figure out how the material's electrons are organized and to model the XAS and XES spectra. By comparing the simulated spectrum to the real spectrum, you can learn about the electronic structure of the object.

- DFT is used to study other properties like optical property, magnetic property of a material. By computing the electronic band structure and density of

states (DOS), DFT is utilized to comprehend a material's optical characteristics. By analyzing the band structure and DOS, it is possible to determine the electronic transitions that give rise to the material's absorption and emission spectra. Other optical characteristics, such the refractive index, and the dielectric function, may be calculated using DFT and are crucial for understanding how light interacts with the material. DFT can measure a material's magnetic moment, which indicates its magnetic field strength. They can calculate magnetic susceptibility, which measures how quickly a substance magnetises in a magnetic field. DFT also study ferromagnetism, antiferromagnetism, and spin glass behaviour.

- DFT is effective in predicting the sensitivity of some nano-structures to environmental pollutants such as sulfur dioxide [87] or acrolein [88], as well as their mechanical characteristics [89].

DFT is also employed in a wide range of other processes, including catalytic reactions, surface property research, and the examination of the electronic compositions of biomolecules, nanoparticles, and nanomaterials. In the grand scheme of things, it can be stated that DFT is an effective technique in the present-day scientific era.

<div align="right">

Chapter 4

</div>

Results and Discussions

4.1   Computational Details

The structural, electronic, and optical properties of $Rb_2NaScCl_6$ double perovskite are studied using the full potential linearized augmented plane wave (FP-LAPW), based on density functional theory method, which is part of the WIEN2k package. The Perdew Burke Ernzerhof (PBE) [90] approximation is used in conjunction with the generalized gradient approximation (GGA) to discover the optimum ground states of the materials under consideration. It has been determined that the minimum values for the radius of the muffin tin (R_{MT}) for Rb, Na, Sc, and Cl are 2.5, 2.5, 2.47, and 2.23 a.u., respectively. We set $RK_{max} = 7$ where R is the smallest radius of muffin-tin sphere and K_{max} is the largest reciprocal lattice vector used in the expansion of flat wave-function. Moreover, the number of k-point is selected to 4000 in Brillouin zone. When the total energy and charge of the system is stable within the energy of 10^{-5} Ry and 10^{-3} e respectively, then self-consistent equation is converged.
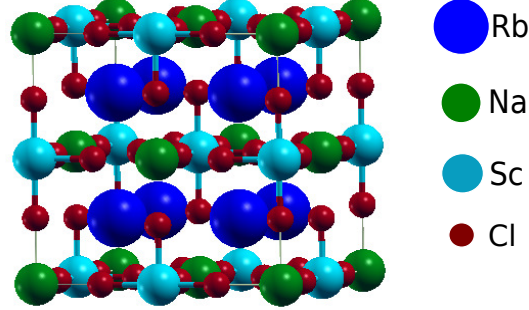
Figure 4.1: Crystal Structure of cubic $Rb_2NaScCl_6$ double perovskite

The volume optimization is provided with WIEN2k package that determines the minimum energy possessed by a system by plotting volume vs energy graph which has been shown in figure 4.2. By volume optimization, the lattice constant has been found to be 10.54793 Å. In order to determine the optimised ground states of the materials being studied, the energy versus volume of a unit cell of the crystals was calculated. The Birch-Murnaghan thermodynamic state relation is used as the basis for this analysis. The relation gives us the following equation [91]:

$$E(\vartheta) = E_o + \frac{9V_0K_0}{16}\left\{\left(\left[\frac{V_0}{V}\right]^{\frac{2}{3}} - 1\right)^3 K_0'\right\} + \frac{9V_0K_0}{16}\left\{\left(\left[\frac{V_0}{V}\right]^{\frac{2}{3}} - 1\right)^2\right\} + \left\{6 - 4\left[\frac{V_0}{V}\right]^{\frac{2}{3}}\right\}$$
(4.1)

Here $E(\vartheta)$ is the energy at volume V, E_0 is the energy at equilibrium volume V_0. The symbol K_0 and K_0' represents the bulk modulus and its derivative respectively. The lattice parameters using different pressures were calculated to see how our compound reacted to the change in pressure and the variation has given in table 4.1. The Birch-Murnaghan equation relates pressure and volume (P-V) and can be expressed in the following form:

$$P = \frac{3}{2}K_0\left[\left(\frac{V_0}{V}\right)^{\frac{7}{3}} - \left(\frac{V_0}{V}\right)^{\frac{5}{3}}\right]\left[1 + \frac{3}{4}(K_0' - 4)\left[\left(\frac{V_0}{V}\right)^{\frac{2}{3}} - 1\right]\right]$$
(4.2)

Results and Discussions
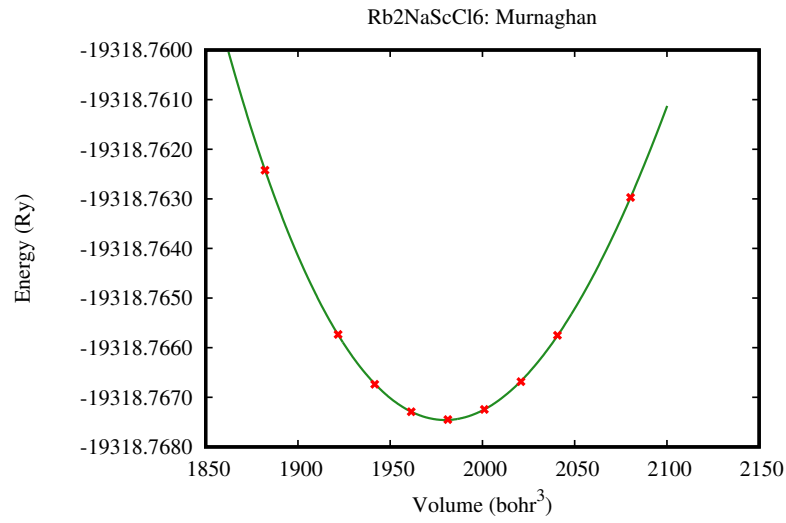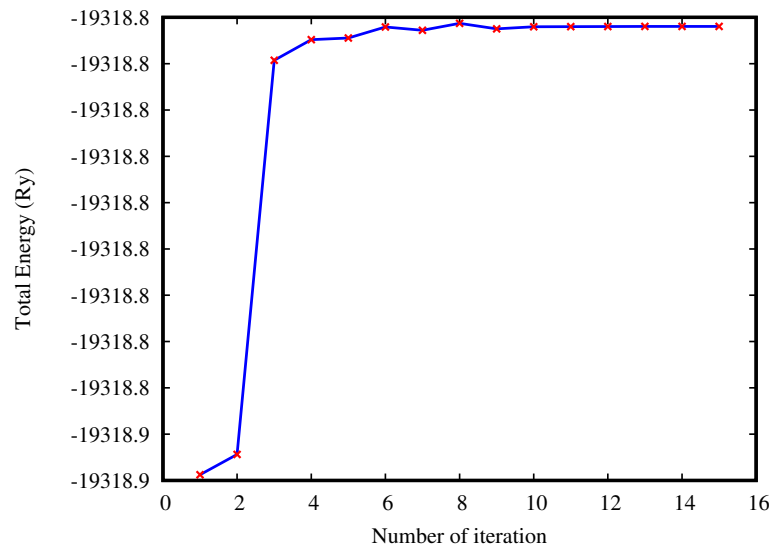
Where K_0 can be represented as follow:

$$K_0 = -V = (\frac{\partial K}{\partial p})_{P=0} \tag{4.3}$$

The total energy, and fermi energy are given in the table has found to be -19318.76195 Ry and -0.0380108 eV respectively. The total energy versus the number of iteration has shown in figure 4.3.

**Figure 4.2:** Energy versus volume optimization curves for $Rb_2NaScCl_6$

Figure 4.3: Energy versus number of iteration curves for $Rb_2NaScCl_6$

4.2   Electronic Properties

4.2.1   Band-Structure

One of our main goals of this project is to generate the band-structure and determine the band-gap of $Rb_2NaScCl_6$ double perovskites. We use the WIEN2k software to generate this band-structure. The input of this calculation is mainly the crystal structure of this metal which is represented in section 1.1. The calculated band-structure of $Rb_2NaScCl_6$ is shown in figure 4.4. The energy gap between the top of the valance band (VB) and the bottom of the conduction band (CB) is founded 3.9 electro volt (eV). So $Rb_2NaScCl_6$ is a compound with a large band-gap. Figure 4.4 shows that the CV minimum and VB maximum are both at the same point Γ. So the crystal has the direct band-gap.
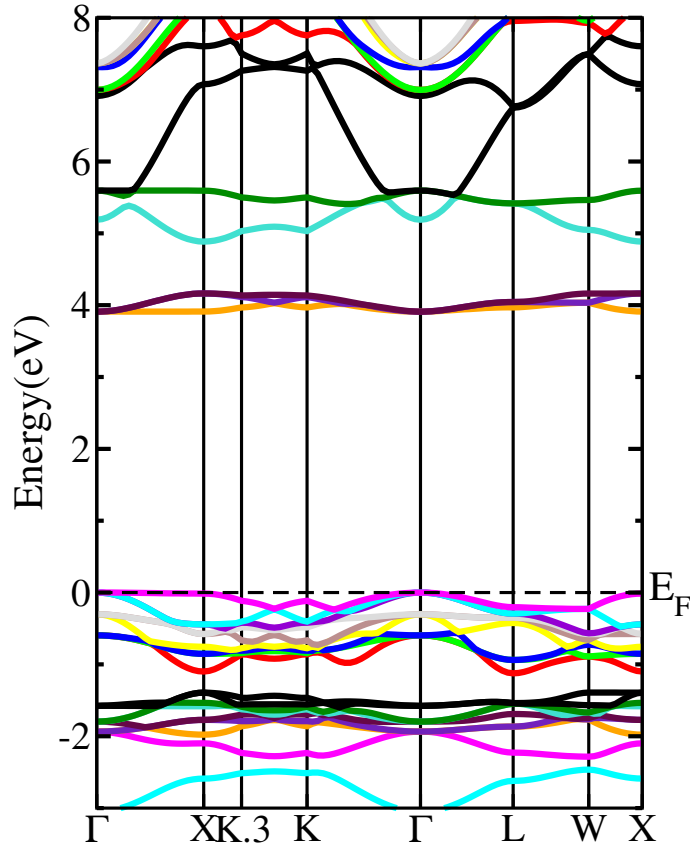
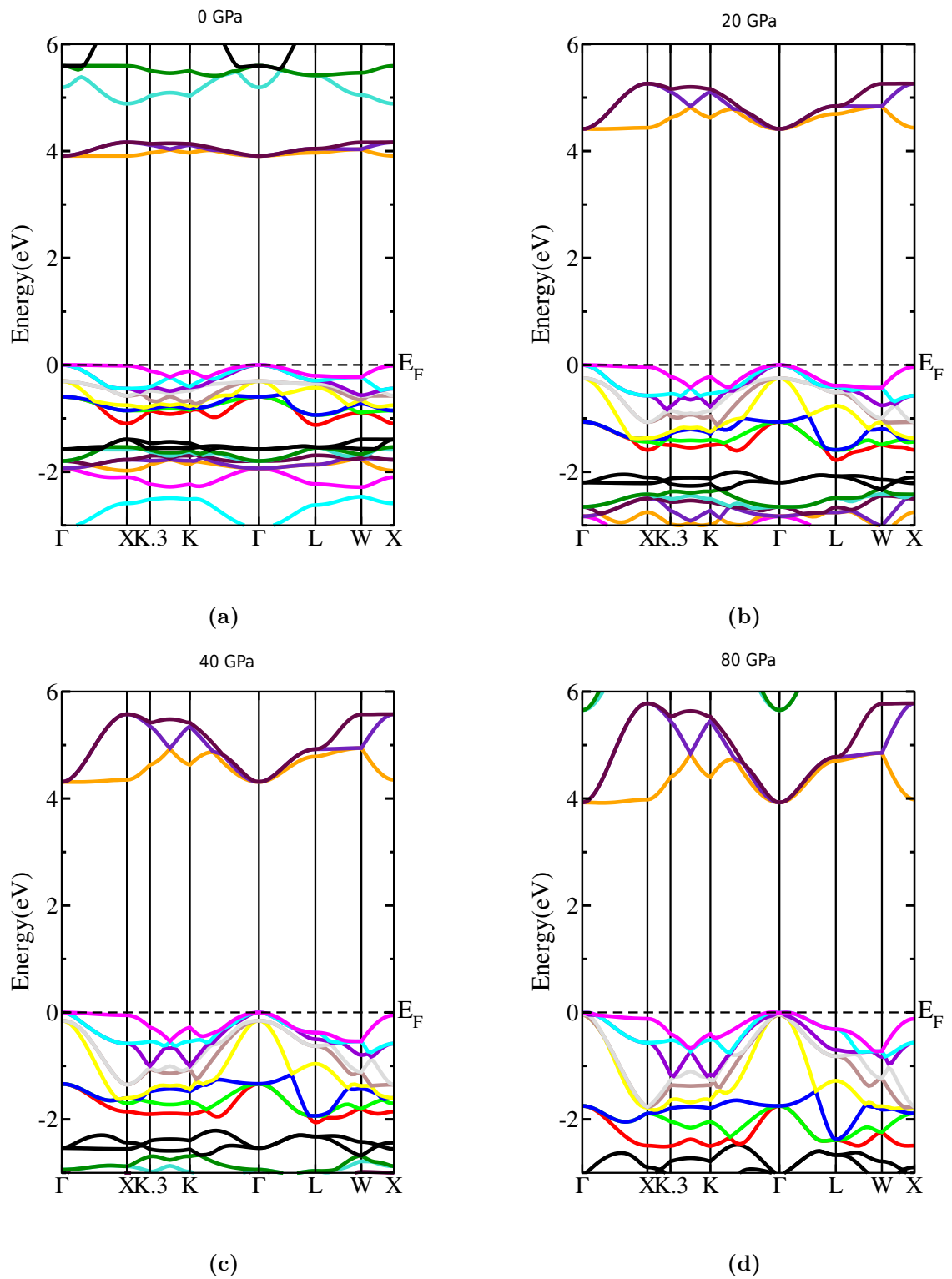**Figure 4.4:** Calculated band structure of $Rb_2NaScCl_6$ using GGA potential

Results and Discussions

We conducted band-gap calculations under varying pressures to investigate the response of our compound to pressure changes. The variation of band-gap under different pressure has shown in table 4.1. According to what is displayed in the table, the lattice constant decrease as the pressure is increased. On the other hand, the band-gap increase till 20 GPa pressure. After that, it begin to decrease. Our compound possesses a property that has the potential to be useful in a variety of important contexts. The band structure of $Rb_2NaScCl_6$ under some of the pressures we examine can be seen in a transparent form in (figures 4.5 and 4.6).

Table 4.1: Change of lattice parameter and band-gap under different pressure

| PRESSURE (GPa)	LATTICE PARAMETER (Å)	BAND-GAP (eV)
0	10.54793	3.908
10	9.80553	4.339
20	9.44203	4.413
30	9.20275	4.378
40	9.02535	4.309
60	8.76893	4.141
80	8.58481	3.919
100	8.44178	3.668
120	8.32516	3.421
140	8.22692	3.186
160	8.14220	2.963
180	8.06780	2.750
200	8.00157	2.549

Figure 4.5: Band structure of Rb$_2$NaScCl$_6$ double perovskite under (a) 0 GPa (b) 20 GPa (c) 40 GPa (d) 80 GPa pressure
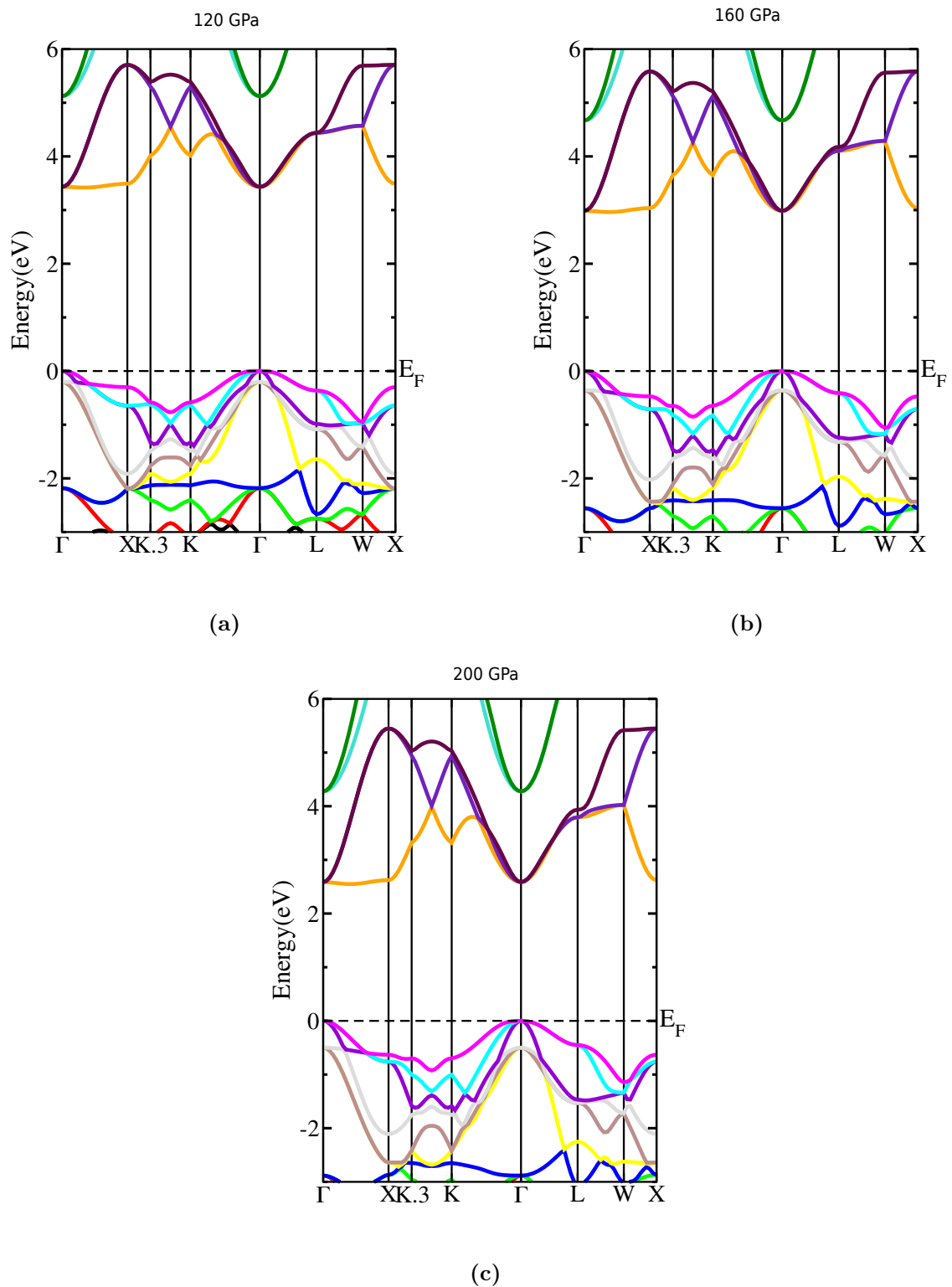
Figure 4.6: Band structure of Rb$_2$NaScCl$_6$ double perovskite under (a) 120 GPa (b) 160 GPa (c) 200 GPa pressure
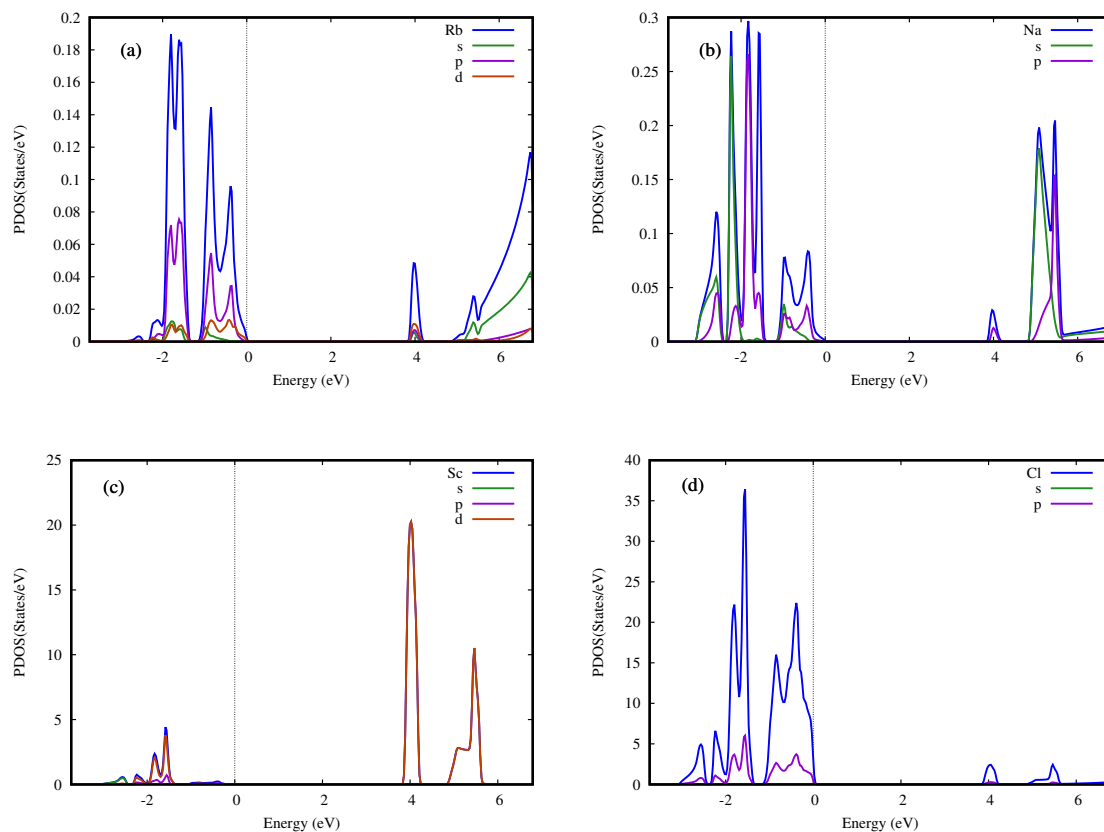
4.2.2 Density of States

The density of states (DOS) of $Rb_2NaScCl_6$ double perovskites is shown in figure 4.7.
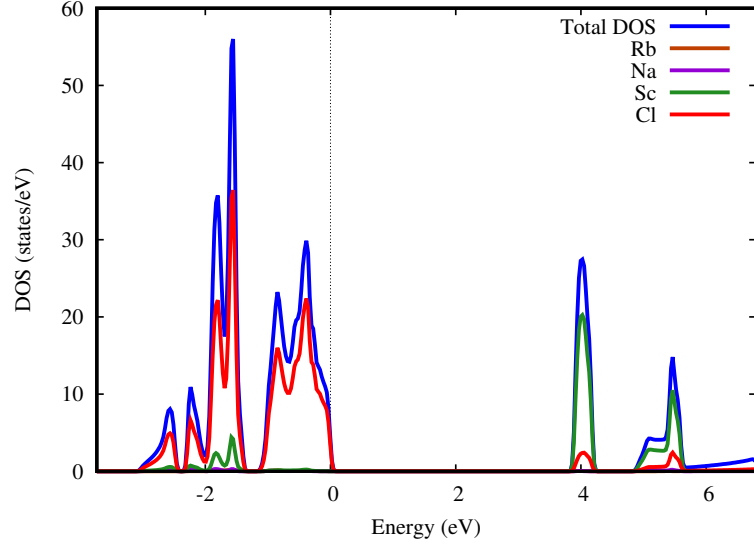
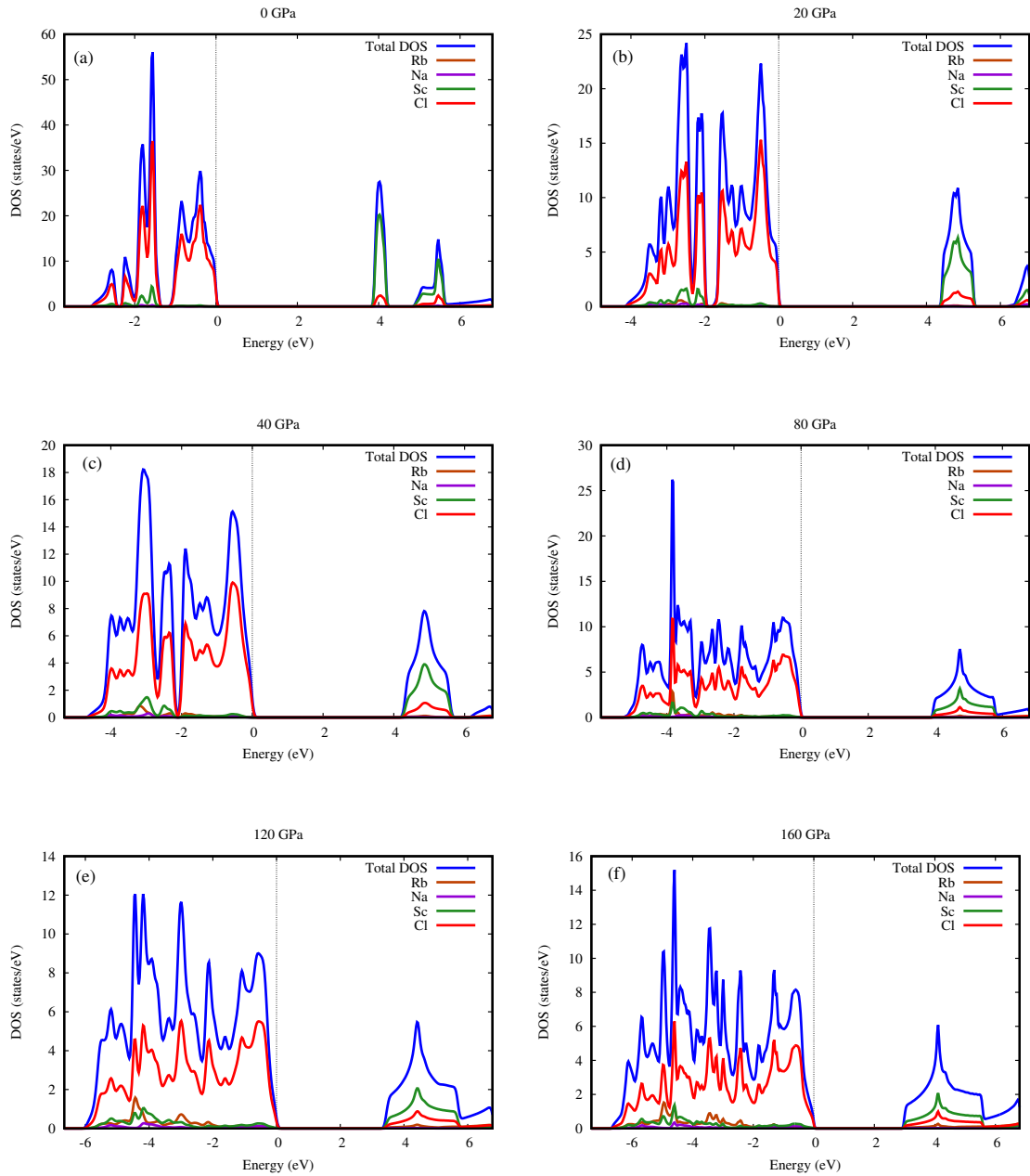**Figure 4.7:** Density of states of $Rb_2NaScCl_6$ double perovskite

The figures for DOS are generated using 20,000 k-points. In total DOS the contribution of Chlorine (Cl) in VB and the contribution of Scandium (Sc) in CB dominates over other atoms. We took the contribution of s, p, d orbitals for Rb and Sc atoms, and s, p orbitals for Na and Cl atoms. The figure 4.8 shows the partial density of states (PDOS) for each atom's orbital. The figure shows that for the Rb atom, the p orbital in VB and s orbital in CB dominate over other orbitals. For the Na atom, both s and p contributes equally in VB. But in CB the s orbital shows slightly large contribution than p. In the Sc atom, the d orbital dominates in both VB and CB. And finally, for Cl atom, both VB and CB are dominated by p orbital. So we can say that p orbital contribution of the Cl atom in VB and d contribution of the Sc atom in CB is more than the other atom's orbital contain in the compound.

Results and Discussions

Figure 4.8: Partial density of states of (a) Rb, (b) Na, (c) Sc, (d) Cl atoms

We create diagrams of the DOS at various pressures. It has been observed that the DOS at the Fermi level changes as the pressure changes. We can relate it with bandgap as the band-gap change as the pressure change. So the energy distance between the VB and CB from fermi level is also change. However, it has been observed that Chlorine and Scandium have made the most significant contributions to the VB and CB, respectively, in every case. The orbitals contribution of all atom has found same as well. The DOS of our compound at different pressure have shown in figure 4.9 and 4.10.

55

Figure 4.9: Density of states of Rb$_2$NaScCl$_6$ double perovskite under (a) 0 GPa (b) 20 GPa (c) 40 GPa (d) 80GPa (e) 120 GPa (f) 160 GPa pressure
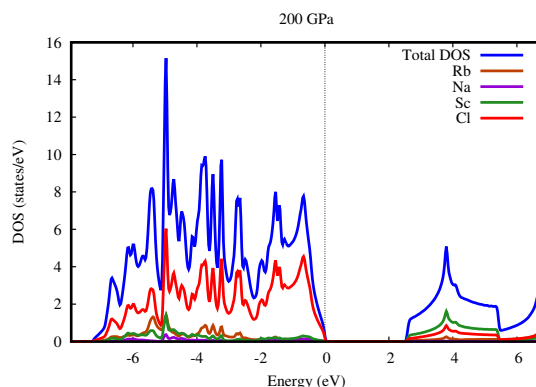
Figure 4.10: Density of states of Rb, Na, Sc, Cl atoms in $Rb_2NaScCl_6$ double perovskite under 200 GPa pressure.

4.3 Optical Properties

4.3.1 Absorption Coefficient

The absorption coefficient is a significant physical property that defines the ability of a material to absorb and reduce the intensity of electromagnetic radiation. In figure 4.11 we can see the variation of absorption coefficient ($10^4/cm$ unit) variation with energy.
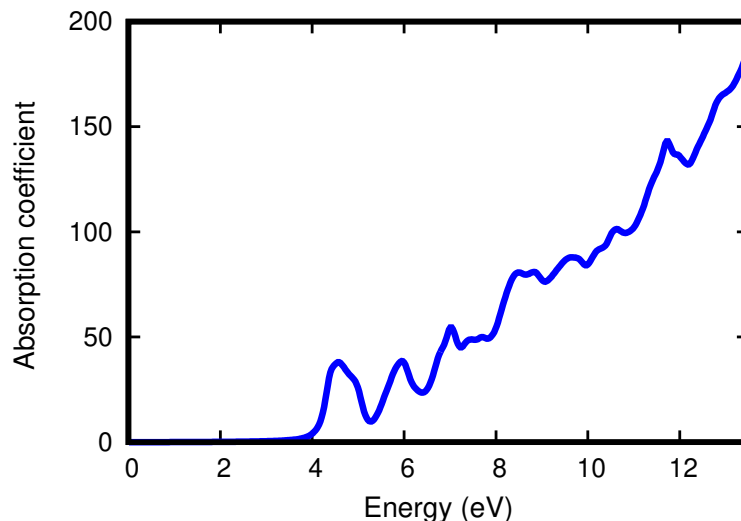
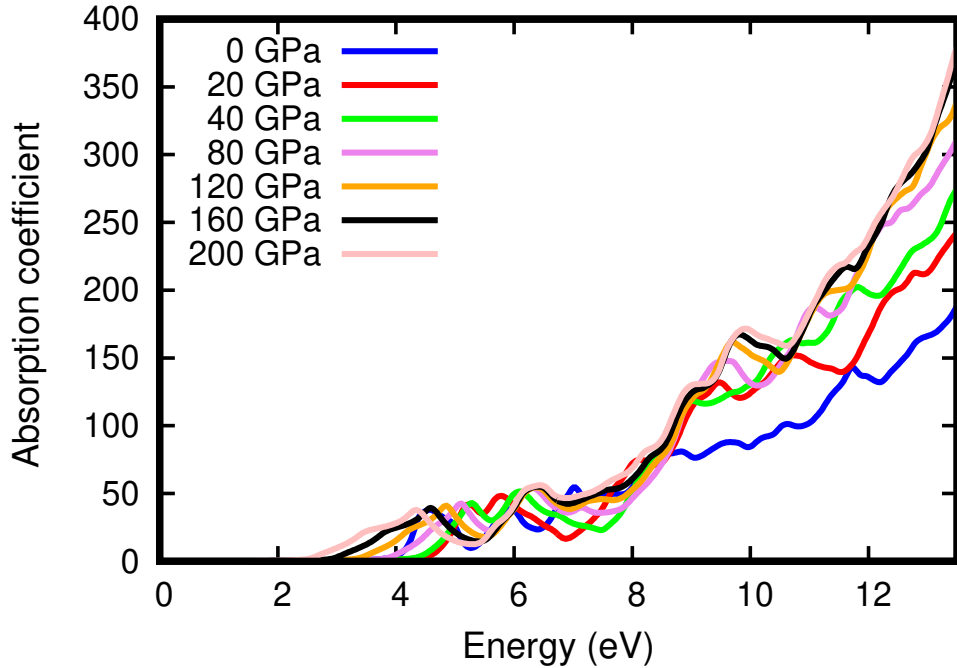**Figure 4.11:** Absorption coefficient figure for $Rb_2NaScCl_6$ double perovskite

Our compound requires a higher energy range to initiate and enhance absorption, due to its wide band-gap. This is because there are no available electronic states

within the band-gap to absorb the incident photons. This implies that there is no absorption of the mentioned light. The absorption coefficient of photons with energies higher than the band-gap varies depending on the wavelength, and is not constant.Visible light has a wavelength that ranges from around 400 to 700 nanometers which is approximately 1.8 to 3 eV in the range of photon energies. For $Rb_2NaScCl_6$, the absorption coefficient in the region of visible light wavelength region is very low. It can be stated that these cannot absorb visible light. However, beyond the region visible light wavelength, there is an increase in absorption, indicating that our compound primarily absorbs ultra-violet light. We model the absorption coefficient diagrams under various pressures. It has been observed that as pressure rises, so does the absorption coefficient in the region of visible light. We can relate this phenomenon with the decreasing of band-gap what we have already observed in section 4.2.1, where the band-gap shrank as pressure increased. The diagrams of absorption coefficient under various pressures can be seen in figure 4.12.

Figure 4.12: Absorption coefficient figure for $Rb_2NaScCl_6$ double perovskite under pressure 0, 20, 40, 80. 120, 160 and 200 GPa
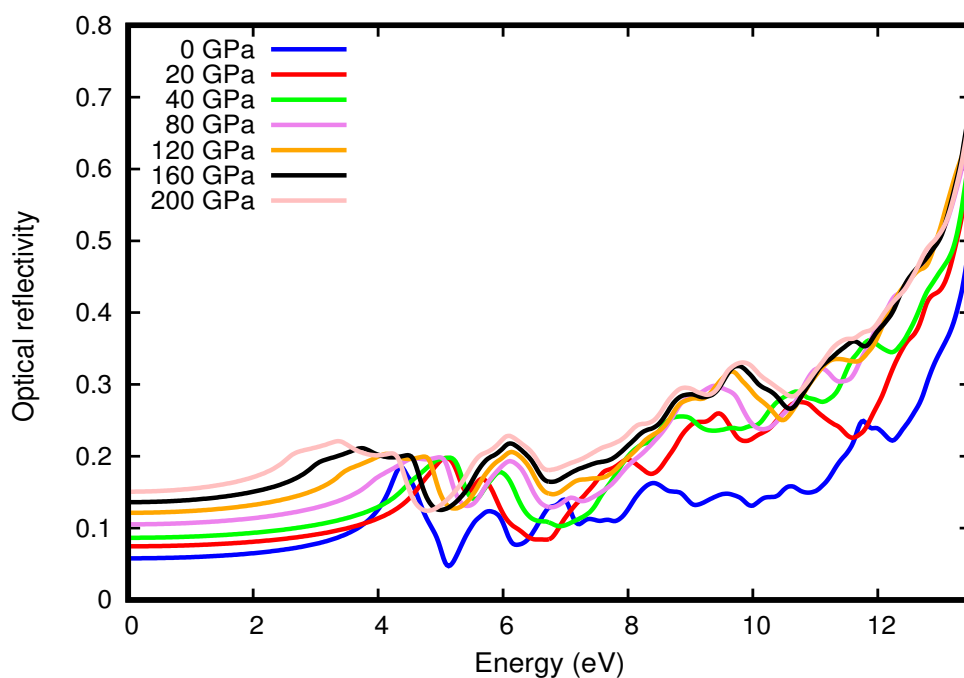
4.3.2   Optical Reflectivity

We are aware that optical reflectivity gauges a material's capacity to reflect light. In figure 4.13 we can see the variation of optical reflectivity with various energy for our material.
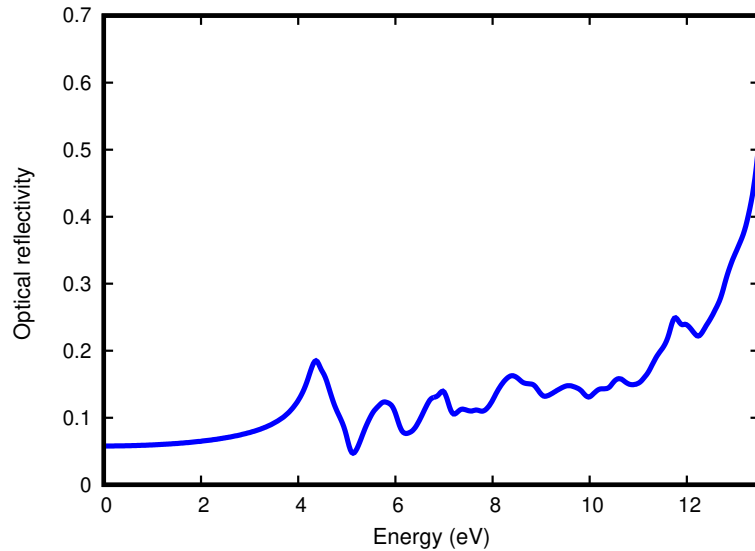
Figure 4.13: Optical reflectivity figure for $Rb_2NaScCl_6$ double perovskite

The figure shows us that under the band-gap energy, the $Rb_2NaScCl_6$ double perovskite has reflectivity of the incident light. After passing through the band-gap energy, it suddenly gives a bigger pick at 4.33 eV energy and move on. The pressure dependency of optical reflectivity for our material has shown in figure 4.14. The figure transparently shows that increasing in a large amount of pressure also increases the initial point of optical reflectivity.

Figure 4.14: Optical reflectivity figure for $Rb_2NaScCl_6$ double perovskite under pressure 0, 20, 40, 80. 120, 160 and 200 GPa
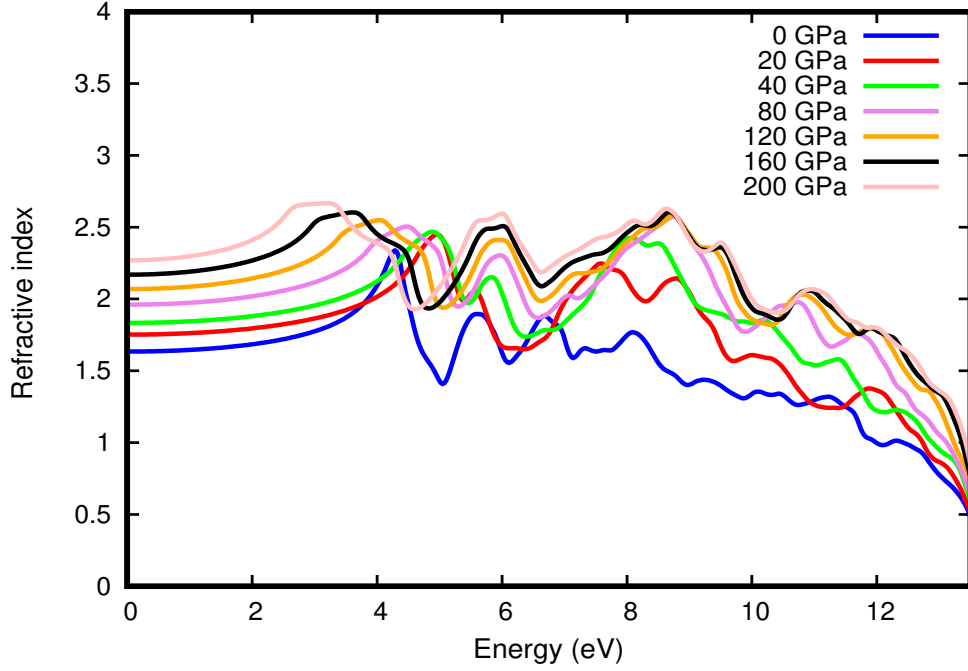
4.3.3 Refractive Index

Figure 4.15 is showing a diagram of refractive index of $Rb_2NaScCl_6$ double perovskite. The graph is showing the relation between correlation between the refractive index and photon energy.
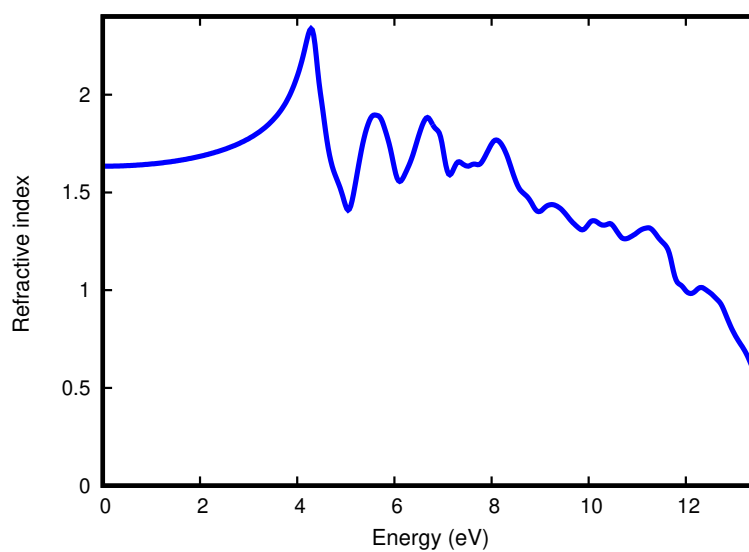
Figure 4.15: Refractive index figure for $Rb_2NaScCl_6$ double perovskite

Results and Discussions

The refractive index is almost constant until we are close to the band energy level. The refractive index is maximum at 4.33 eV energy. So, in the UV regions, the compound is transparent. After 8 eV the refractive index is continuously decreasing. The change between the refractive index and photon energy under different pressure has shown in figure 4.16.
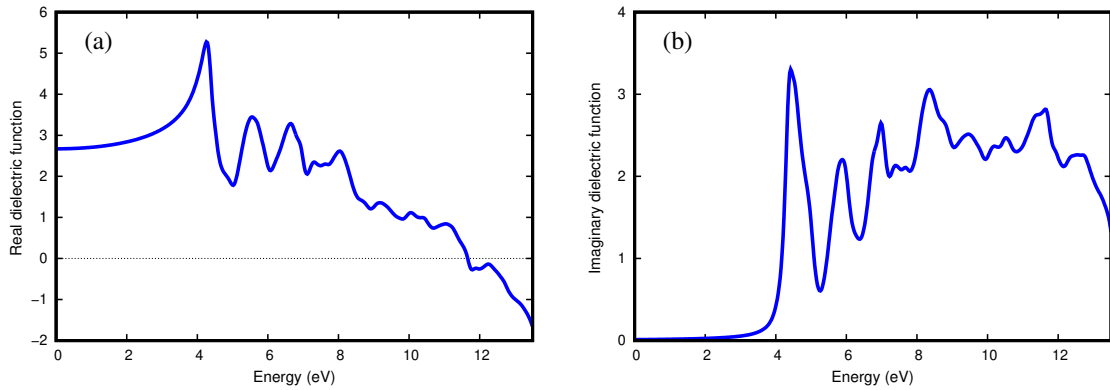

Figure 4.16: Refractive index figure for $Rb_2NaScCl_6$ double perovskite under pressure 0, 20, 40, 80. 120, 160 and 200 GPa

4.3.4 Dielectric Function

The dielectric function component for face centered cubic crystal $Rb_2NaScCl_6$ have illustrated in the figure 4.17. In the diagram we can see the variation of both real and imaginary part dielectric function with respect to energy. Both of the part have shown a static movement from two different initial point until band energy. The imaginary part of dielectric function, which is related to the material's absorption of electromagnetic radiation, starts to increase after band-gap energy and has its highest pick point at 4.45 eV energy. It is because at energies that are much higher than the band-gap, the material absorb a lot of energy, and the imaginary part of the dielectric function will be the most important. On the other hand, the real part

60

which has its highest pick point at 4.27 eV and than it starts going downward. At high energies, the real part of the dielectric function goes to zero, which means that the material acts like a conductor.

Figure 4.17: (a) Real and (b) imaginary part of dielectric function for $Rb_2NaScCl_6$ double perovskite

The pressure dependency of $Rb_2NaScCl_6$ double perovskite has shown in figure 4.18 and 4.19.
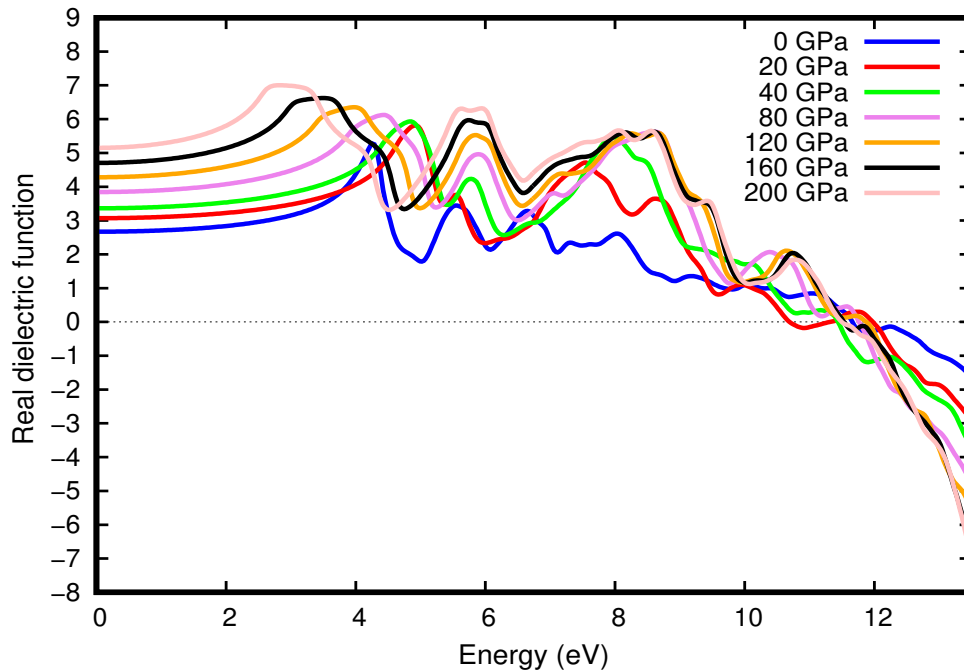
Figure 4.18: Real dielectric function figure for $Rb_2NaScCl_6$ double perovskite under pressure 0, 20, 40, 80. 120, 160 and 200 GPa
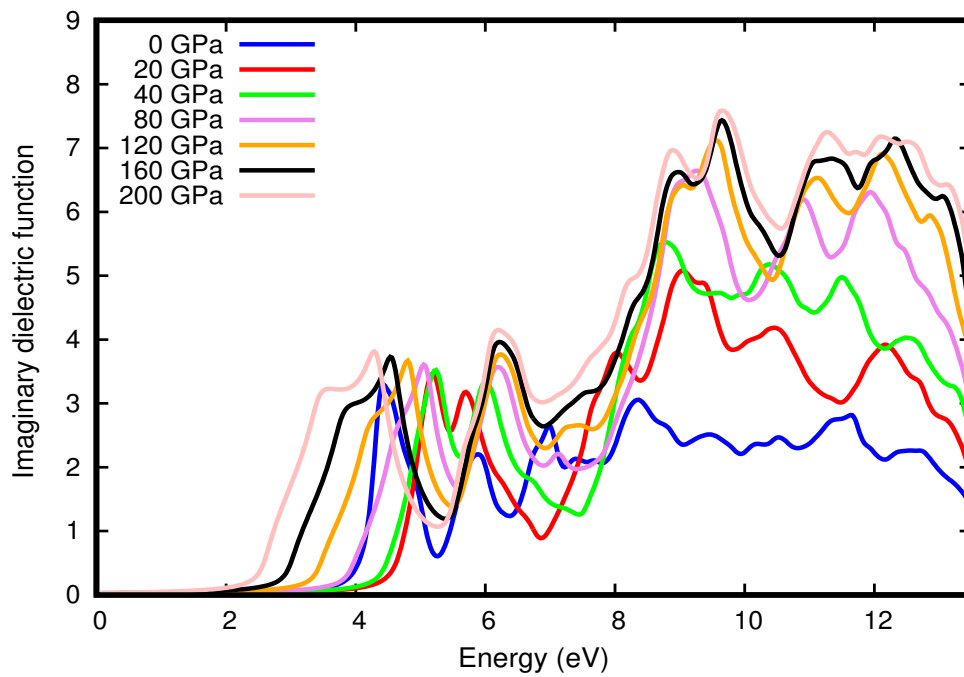
Figure 4.19: Imaginary dielectric function figure for $Rb_2NaScCl_6$ double perovskite under pressure 0, 20, 40, 80. 120, 160 and 200 GPa

4.3.5 Optical Conductivity

The diagram for optical conductivity ($\Omega^{-1}cm^{-1}$ unit), which describes how well a material conducts electricity in response to an applied electric field of our material $Rb_2NaScCl_6$ shown in figure 4.13:
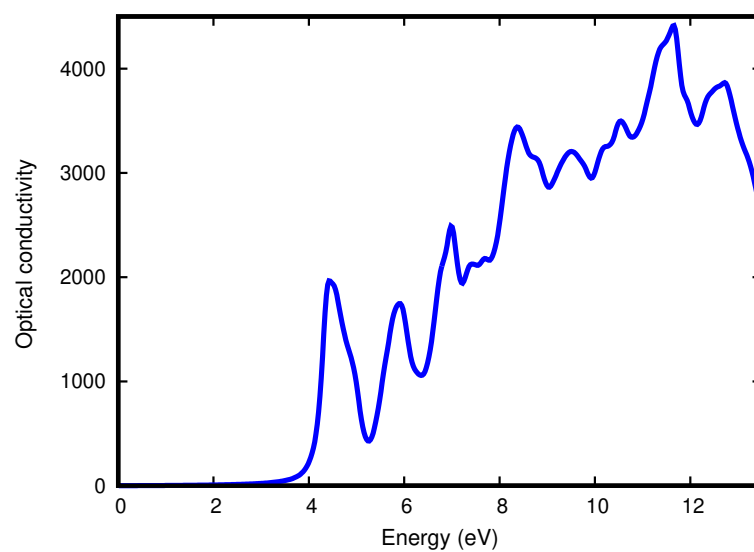
Figure 4.20: Optical conductivity figure of $Rb_2NaScCl_6$ double perovskite

Results and Discussions

The figure shows us that after crossing the bang-gap energy in x-axis, the conductivity of our compound starts increasing. This is so that it can excite its electrons from VB to CB after receiving this level of energy. As a result, the CB in the material gains free electrons, enabling electrical conductivity. It have the highest conductivity at energy 12 eV. After passing energy 13 eV, the conductivity starts falling to the bottom. The pressure dependency of $Rb_2NaScCl_6$ double perovskite has shown figure 4.21. The figure clearly demonstrates that as pressure increases, the optical conductivity of the material also increases.
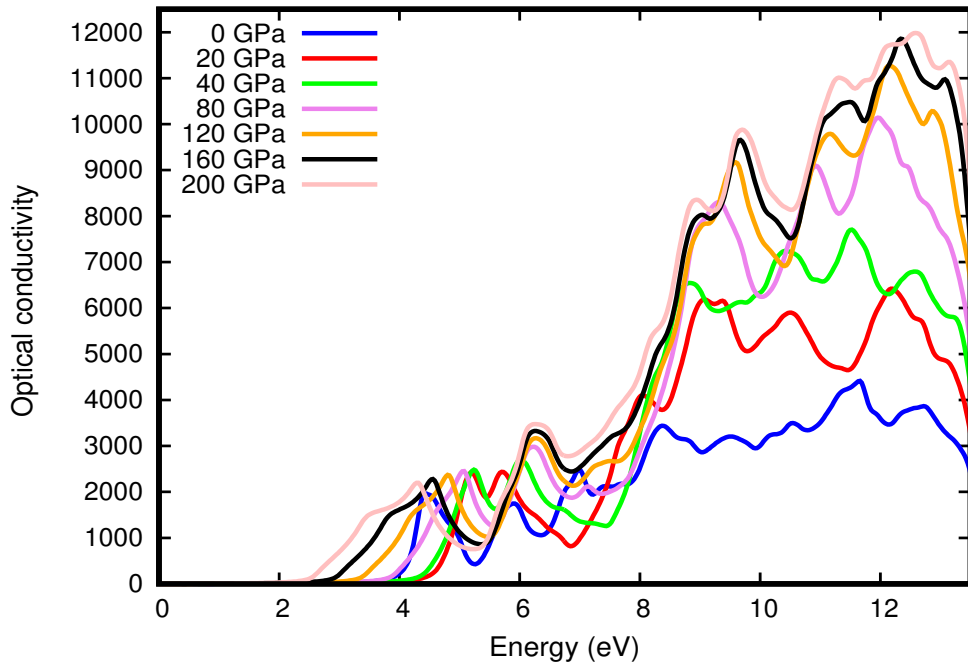
Figure 4.21: Optical conductivity figure for $Rb_2NaScCl_6$ double perovskite under pressure 0, 20, 40, 80. 120, 160 and 200 GPa

4.3.6 Electron Energy Loss

Electron energy loss (EEL) refers to the amount of energy that an electron loses while traversing a substance.The plot for EEL for $Rb_2NaScCl_6$ double perovskite has been shown in figure 4.22.
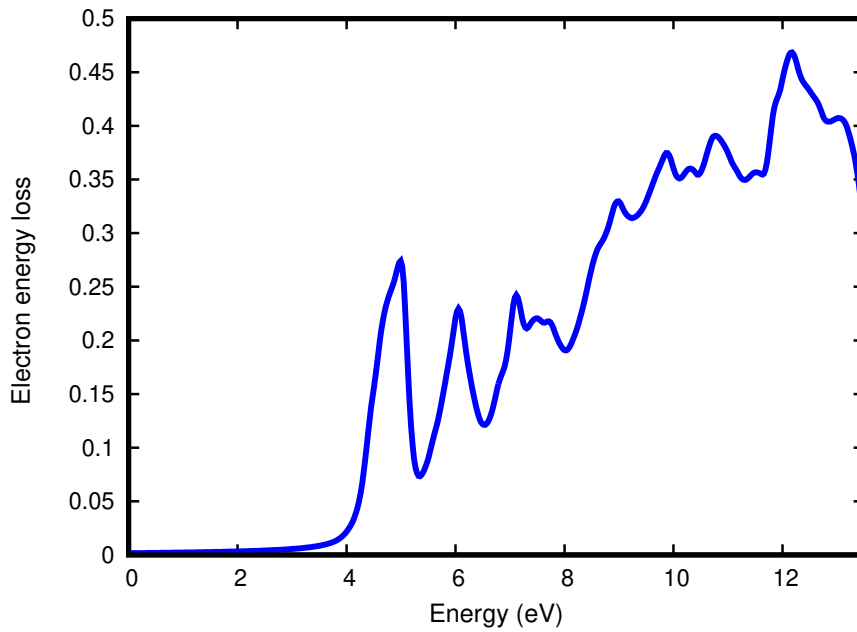
Figure 4.22: Electron energy loss figure for $Rb_2NaScCl_6$ double perovskite

The figure demonstrates that as electron energy rises, so does its EEL. This happens because the electrons and atoms in the compound interact. As a result, the electrons to give up energy via things like excitation and ionization. There is presence of multiple pick in different energy level. It is because of appearance of different atoms in our compound. From the plot for different pressure, we can see from figure 4.23 that EEL starts more early energy than it's lower pressure. But the the pick points EEL also decrease as well.
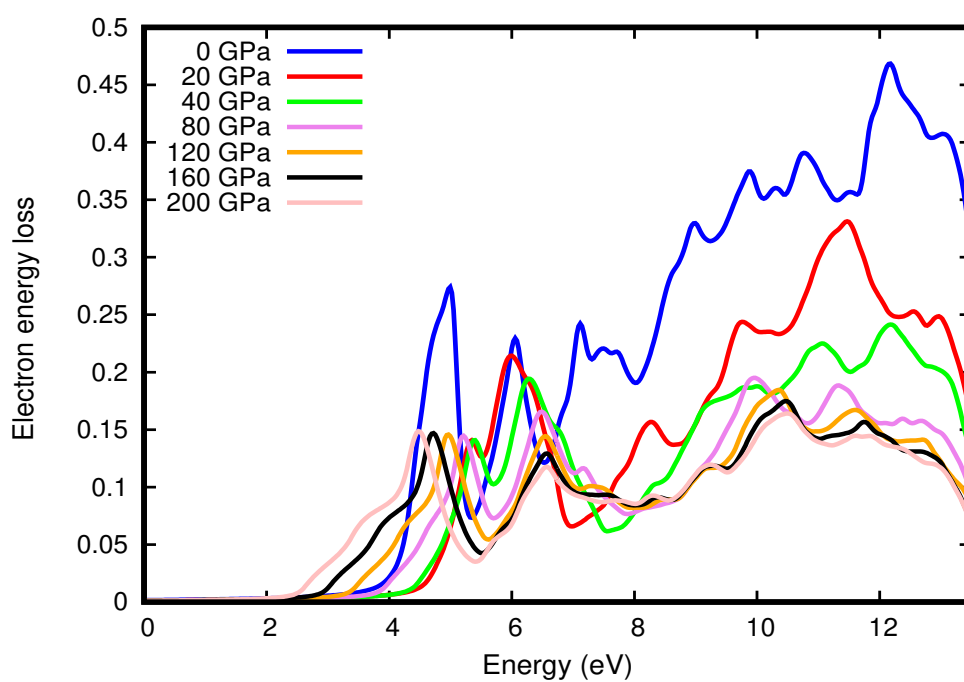
Figure 4.23: Electron energy loss figure for Rb$_2$NaScCl$_6$ double perovskite under pressure 0, 20, 40, 80. 120, 160 and 200 GPa

<div align="right">

Chapter 5

</div>

Conclusion

5.1   Summery of Results

The crystal structure of the material $Rb_2NaScCl_6$ double perovskite has been analyzed, and its electronic and optical properties have been determined through our study. The lattice parameter has been determined to be 10.54793 Å. The band-gap is found to be 3.9 eV, and it has been determined that the material exhibits direct band-gap characteristics. It was observed that chlorine has a significant contribution in the VB, while scandium dominates in the CB compared to other atoms. The optical properties are significantly influenced by the band-gap. For example, we have a material with a wide band-gap that mostly absorbs UV light because low energy and long wave lengths can't move an electron from the valence band to the conduction band. Increasing the energy level of the material can enhance certain characteristics such as conductivity, imaginary dielectric function, and electron energy loss. However, the process also amplify the reduction of other characteristics such as the refractive index.

The study shows the material characteristics at different levels of pressure. The results indicate a reduction in lattice parameter. The value of the band-gap increases until a pressure of 20 GPa is reached. Following that, the band-gap starts to put

down as pressure builds. The contribution of atoms in DOS was discovered to be the same regardless of pressure. The equivalence of the contribution of chlorine and scandium in the VB and CB has been observed to remain consistent with previous findings. The optical characteristics have been observed to undergo alterations in response to variations in pressure. For example, figure 4.18 and 4.19 demonstrate that raising the pressure can result in an increase in the imaginary dielectric function, while causing a decrease in the real dielectric function at high energy levels. As the pressure increases, there is a shift in the starting point of the absorption coefficient from the UV to the visible range of wavelength in the electromagnetic spectrum. The other optical properties are also influenced by the changes in pressure.

5.2   Scope of Future Applications

Energy consumption is rising with time in today's globe. Third-world countries struggling to satisfy their basic demand for energy. Renewable energy, like solar cells, water splitting will be a simple and elegant answer to these problems. Solar panel needs materials that can absorb visible light and convert the light into electrical current. Regrettably, the material $Rb_2NaScCl_6$ exhibits a broad band-gap, which precludes its capacity to absorb the visible light. However, there are opportunities to reduce the band-gap of the material through the process of doping. Numerous experiments have demonstrated that the utilization of an appropriate doping material can result in a reduction of the band-gap of double perovskite [92–94]. Additionally, if the material's band-gap is narrowed, it can be used to make optical devices like lasers and LEDs. Moreover, through appropriate composition, a direct bandgap material with a wide band-gap can be readily employed for the process of water splitting [95, 96]. The transition-metal sites can act as an active sites where different reaction can take place. Using this nature we can use it multiple purpose like catalysis. Because this material absorb UV light very well, it can be used to make devices such as optical filter devices and water purification devices.

$Rb_2NaScCl_6$ has potential to use it for Tandem solar cells [97], which is a new technology for the future. The word "Tandem" refers to multi-junction. A tandem solar

cell is a device that has multiple layers of different compounds featuring various band-gaps piled on top of one another. Each layer can absorb a different part of the solar spectrum. This makes it easier to absorb sunlight and increase the efficiency of the conversion. In this case, the high-energy photons that are not absorbed by the lower layers would be taken in by the wide band-gap material. The solar cell's overall performance would get up as a result. The material is devoid of hazardous elements such as Mercury (Hg), Lead (Pb), Arsenic (As), and others listed in the periodic table. This renders the compound harmless to the environment. This material can be applied without concern for potential harm to both human health and the environment.

In summary, it can be stated that with appropriate utilization, $Rb_2NaScCl_6$ compound can serve multiple purposes, including energy consumption applications.

Appendix

Functional

In our description of density functional theory, we use the term functional. What does "functional" mean? A functional is a operation that takes a function as the input and produces a single number as the result. So in a functional, one function is basically said to be mapped into another. For example we consider a functional $F[f(x)]$ such that :

$$F[f(x)] = \int_{-1}^{1} f(x)dx \tag{5.1}$$

Where, the function $f(x)$ is $(x^2 + 1)$. By evaluating further, we obtain:

$$F[f(x)] = \int_{-1}^{1} (x^2 + 1)dx = \int_{-1}^{1} x^2 dx + \int_{-1}^{1} 1 dx = \frac{x^3}{3}\Big|_{-1}^{1} + x\Big|_{-1}^{1} = \frac{8}{3} \tag{5.2}$$

So we get an output of a single number. In DFT, the most important function is energy functional $E[n(\vec{r})]$. Employing the electronic density, it figures out the energy of the whole machine.

Bibliography

[1] Nathan S Lewis and Daniel G Nocera. Powering the planet: Chemical challenges in solar energy utilization. *PNAS*, 103(43):15729–15735, 2006.

[2] Daniel G Nocera. Solar fuels and solar chemicals industry. *Acc. Chem. Res.*, 50(3):616–619, 2017.

[3] Huanping Zhou, Qi Chen, Gang Li, Song Luo, Tze-bing Song, Hsin-Sheng Duan, Ziruo Hong, Jingbi You, Yongsheng Liu, and Yang Yang. Interface engineering of highly efficient perovskite solar cells. *Science*, 345(6196):542–546, 2014.

[4] Julian Burschka, Norman Pellet, Soo-Jin Moon, Robin Humphry-Baker, Peng Gao, Mohammad K Nazeeruddin, and Michael Grätzel. Sequential deposition as a route to high-performance perovskite-sensitized solar cells. *Nature*, 499(7458):316–319, 2013.

[5] Christopher Eames, Jarvist M Frost, Piers RF Barnes, Brian C O'regan, Aron Walsh, and M Saiful Islam. Ionic transport in hybrid lead iodide perovskite solar cells. *Nat. Commun.*, 6(1):7497, 2015.

[6] Shammya Afroze, AfizulHakem Karim, Quentin Cheok, Sten Eriksson, and Abul K Azad. Latest development of double perovskite electrode materials for solid oxide fuel cells: a review. *Front. Energy*, 13:770–797, 2019.

[7] Zhenhua Weng, Jiajun Qin, Akrajas Ali Umar, Jiao Wang, Xin Zhang, Haoliang Wang, Xiaolei Cui, Xiaoguo Li, Lirong Zheng, and Yiqiang Zhan. Lead-free cs2biagbr6 double perovskite-based humidity sensor with superfast recovery time. *Adv. Funct. Mater.*, 29(24):1902234, 2019.

[8] Tong Liu, Tong Wang, Hangfei Li, Jie Su, Xidong Hao, Fengmin Liu, Fangmeng Liu, and Xishuang Liang. Ethanol sensor using gadolinia-doped ceria solid

electrolyte and double perovskite structure sensing material. *Sens. Actuators B Chem.*, 349:130771, 2021.

[9] Xiaomin Xu, Yijun Zhong, and Zongping Shao. Double perovskites in catalysis, electrocatalysis, and photo (electro) catalysis. *Trends Chem.*, 1(4):410–424, 2019.

[10] Feroz A Najar, Shohaib Abass, Khalid Sultan, Mubashir A Kharadi, Gul Faroz A Malik, and Rubiya Samad. Comparative study of optical properties of substitutionally doped la2nimno6 double perovskite ceramic: A potential candidate for solar cells and dielectrics. *Physica B: Condensed Matter*, 621:413311, 2021.

[11] Akihiro Kojima, Kenjiro Teshima, Yasuo Shirai, and Tsutomu Miyasaka. Organometal halide perovskites as visible-light sensitizers for photovoltaic cells. *J. Am. Chem. Soc.*, 131(17):6050–6051, 2009.

[12] Woon Seok Yang, Jun Hong Noh, Nam Joong Jeon, Young Chan Kim, Seungchan Ryu, Jangwon Seo, and Sang Il Seok. High-performance photovoltaic perovskite layers fabricated through intramolecular exchange. *Science*, 348(6240):1234–1237, 2015.

[13] Xiaojun Qin, Zhiguo Zhao, Yidan Wang, Junbo Wu, Qi Jiang, and Jingbi You. Recent progress in stability of perovskite solar cells. *J. Semicond.*, 38(1):011002, 2017.

[14] Pradeep R Varadwaj. A 2 agcrcl 6 (a= li, na, k, rb, cs) halide double perovskites: a transition metal-based semiconducting material series with appreciable optical characteristics. *Phys. Chem. Chem. Phys.*, 22(42):24337–24350, 2020.

[15] NA Noor, M Waqas Iqbal, Taharh Zelai, Asif Mahmood, HM Shaikh, Shahid M Ramay, and Waheed Al-Masry. Analysis of direct band gap a2scini6 (a= rb, cs) double perovskite halides using dft approach for renewable energy devices. *J. Mater. Res. Technol.*, 13:2491–2500, 2021.

[16] Hongwei Lei, David Hardy, and Feng Gao. Lead-free double perovskite cs2agbibr6: fundamentals, applications, and perspectives. *Adv. Funct. Mater.*, 31(49):2105898, 2021.

[17] Hui Chen, Hang Lin, Qingming Huang, Feng Huang, Ju Xu, Bo Wang, Zebin Lin, Jiangcong Zhou, and Yuansheng Wang. A novel double-perovskite gd 2

zntio 6: Mn 4+ red phosphor for uv-based w-leds: structure and luminescence properties. *J. Mater. Chem. C*, 4(12):2374–2381, 2016.

[18] Bingjie Han, Jing Ren, PingPing Teng, JiaBao Zhu, Yu Shen, ZhiAng Li, Xiaoliang Zhu, and Xinghua Yang. Synthesis and photoluminescence properties of a novel double perovskite ca2lasbo6: Sm3+ phosphor for w-leds. *Ceram. Int.*, 48(1):971–980, 2022.

[19] Quan Liu, Xibing Li, Bing Zhang, Lixi Wang, Qitu Zhang, and Le Zhang. Structure evolution and delayed quenching of the double perovskite nalamgwo6: Eu3+ phosphor for white leds. *Ceram. Int.*, 42(14):15294–15300, 2016.

[20] Kang Yi, Qingkai Tang, Zhiwei Wu, and Xinhua Zhu. Unraveling the structural, dielectric, magnetic, and optical characteristics of nanostructured la2nimno6 double perovskites. *Nanomaterials*, 12(6):979, 2022.

[21] DD Sarma, EV Sampathkumaran, Sugata Ray, R Nagarajan, Subham Majumdar, Ashwani Kumar, G Nalini, and TN Guru Row. Magnetoresistance in ordered and disordered double perovskite oxide, sr2femoo6. *Solid State Commun.*, 114(9):465–468, 2000.

[22] Md Saiduzzaman, Takahiro Takei, and Nobuhiro Kumada. Hydrothermal magic for the synthesis of new bismuth oxides. *Inorg. Chem. Front.*, 8(11):2918–2938, 2021.

[23] Sanjeev Kumar, Gianluca Giovannetti, Jeroen van den Brink, and Silvia Picozzi. Theoretical prediction of multiferroicity in double perovskite y 2 nimno 6. *Phys. Rev. B*, 82(13):134429, 2010.

[24] Q. Mahmood, T. Ghrib, A. Rached, A. Laref, and M.A. Kamran. Probing of mechanical, optical and thermoelectric characteristics of double perovskites cs2gecl/br6 by dft method. *Mater Sci Semicond Process*, 112:105009, 2020.

[25] N.A. Noor, M. Waqas Iqbal, Taharh Zelai, Asif Mahmood, H.M. Shaikh, Shahid M. Ramay, and Waheed Al-Masry. Analysis of direct band gap a2scini6 (a=rb, cs) double perovskite halides using dft approach for renewable energy devices. *J. Mater. Res. Technol.*, 13:2491–2500, 2021.

[26] Muhammad Saeed, Izaz Ul Haq, Awais Siddique Saleemi, Shafiq Ur Rehman, Bakhtiar Ul Haq, Aijaz Rasool Chaudhry, and Imad Khan. First-principles

prediction of the ground-state crystal structure of double-perovskite halides cs2agcrx6 (x = cl, br, and i). *J Phys Chem Solids*, 160:110302, 2022.

[27] K-I Kobayashi, T Kimura, H Sawada, K Terakura, and Y Tokura. Room-temperature magnetoresistance in an oxide material with an ordered double-perovskite structure. *Nature*, 395(6703):677–680, 1998.

[28] Loreta A Muscarella and Eline M Hutter. Halide double-perovskite semiconductors beyond photovoltaics. *ACS Energy Lett.*, 7(6):2128–2135, 2022.

[29] Victor Moritz Goldschmidt. Die gesetze der krystallochemie. *Naturwissenschaften*, 14(21):477–485, 1926.

[30] Chonghe Li, Kitty Chi Kwan Soh, and Ping Wu. Formability of abo3 perovskites. *J. Alloys Compd.*, 372(1-2):40–48, 2004.

[31] Chonghe Li, Kitty Chi Kwan Soh, and Ping Wu. Formability of abo3 perovskites. *J. Alloys Compd.*, 372(1-2):40–48, 2004.

[32] Chonghea Li, Xionggang Lu, Weizhong Ding, Liming Feng, Yonghui Gao, and Ziming Guo. Formability of abx3 (x= f, cl, br, i) halide perovskites. *Acta Crystallogr. Section B: Structural Science*, 64(6):702–707, 2008.

[33] Mosayeb Naseri, Dennis R Salahub, Shirin Amirian, Hatef Shahmohamadi, Mohammad Abdur Rashid, Mehrdad Faraji, and Negin Fatahi. Multi-functional lead-free ba2xsbo6 (x= al, ga) double perovskites with direct bandgaps for photocatalytic and thermoelectric applications: A first principles study. *Mater. Today Commun.*, 35:105617, 2023.

[34] Charles Kittel and Paul McEuen. *Introduction to solid state physics*. John Wiley & Sons, 2018.

[35] Ben G Streetman and Sanjay Kumar Banerjee. *Solid state electronic devices: Global edition*. Pearson education, 2016.

[36] KJ Dean. Waves and fields in optoelectronics: Prentice-hall series in solid state physical electronics, 1984.

[37] Michael P Marder. *Condensed matter physics*. John Wiley & Sons, 2010.

[38] James Deane Patterson and Bernard C Bailey. *Solid-state physics: introduction to the theory*. Springer Science & Business Media, 2007.

Bibliography

[39] Iftikhar Ahmad, B Amin, M Maqbool, S Muhammad, G Murtaza, S Ali, and NA Noor. Optoelectronic response of gezn2o4 through the modified becke—johnson potential. *Chin. Phys. Lett.*, 29(9):097102, 2012.

[40] B Amin, Iftikhar Ahmad, M Maqbool, Souraya Goumri-Said, and R Ahmad. Ab initio study of the bandgap engineering of al 1- x ga x n for optoelectronic applications. *J. Appl. Phys.*, 109(2):023109, 2011.

[41] F Wooten. Optical properties of solids academic press: New york. *NY, USA, London, UK*, 1972.

[42] . F. wooten: Optical properties of solids, academic press, new york and london, 1972, 260 , 23.5× 16cm, 4,660 . , 28(9):803–804, 1973.

[43] E Weingartner, H Saathoff, M Schnaiter, N Streit, B Bitnar, and U Baltensperger. Absorption of light by soot particles: determination of the absorption coefficient by means of aethalometers. *J. Aerosol Sci.*, 34(10):1445–1463, 2003.

[44] Feroz A Najar, Shohaib Abass, Khalid Sultan, Mubashir A Kharadi, Gul Faroz A Malik, and Rubiya Samad. Comparative study of optical properties of substitutionally doped la2nimno6 double perovskite ceramic: A potential candidate for solar cells and dielectrics. *Physica B: Condensed Matter*, 621:413311, 2021.

[45] Luyan Li, Weihua Wang, Hui Liu, Xindian Liu, Qinggong Song, and Shiwei Ren. First principles calculations of electronic band structure and optical properties of cr-doped zno. *J. Phys. Chem. C*, 113(19):8460–8464, 2009.

[46] DP Rai, A Shankar, MP Ghimire, RK Thapa, et al. The electronic, magnetic and optical properties of double perovskite a2fereo6 (a= sr, ba) from first principles approach. *Comput. Mater. Sci.*, 101:313–320, 2015.

[47] Robert G Parr and Weitao Yang. Density-functional theory of the electronic structure of molecules. *Annu. Rev. Phys. Chem.*, 46(1):701–728, 1995.

[48] Walter Kohn. Nobel lecture: Electronic structure of matter—wave functions and density functionals. *Rev. Mod. Phys.*, 71(5):1253, 1999.

[49] Erwin Schrödinger. An undulatory theory of the mechanics of atoms and molecules. *Phys. Rev.*, 28(6):1049, 1926.

Bibliography

[50] Stefaan Cottenier et al. Density functional theory and the family of (l) apw-methods: a step-by-step introduction. *Instituut voor Kern-en Stralingsfysica, KU Leuven, Belgium*, 4(0):41, 2002.

[51] Paul Adrien Maurice Dirac. Quantum mechanics of many-electron systems. *Proceedings of the Royal Society of London. Series A, Containing Papers of a Mathematical and Physical Character*, 123(792):714–733, 1929.

[52] SHREEMOYEE GANGULY. A study of the effect of disorder and confinement on binary systems. 2011.

[53] Darrell F Schroeter. Introductiontoq ua ntummechanics. 2016.

[54] Wolfgang Pauli. The connection between spin and statistics. *Phys. Rev.*, 58(8):716, 1940.

[55] Arthur Jabs. Connecting spin and statistics in quantum mechanics. *Found Phys*, 40:776–792, 2010.

[56] Yu Yu Rusakov and Leonid Borisovich Krivdin. Modern quantum chemical methods for calculating spin–spin coupling constants: theoretical basis and structural applications in chemistry. *Russ. Chem. Rev.*, 82(2):99–130, 2013.

[57] Nouredine Zettili. Quantum mechanics: concepts and applications, 2003.

[58] Klaus Capelle. A bird's-eye view of density-functional theory. *Braz. J. Phys.*, 36:1318–1343, 2006.

[59] Jorge Kohanoff. *Electronic structure calculations for solids and molecules: theory and computational methods*. Cambridge university press, 2006.

[60] Niklas Zwettler. Density functional theory.

[61] Douglas R Hartree. The wave mechanics of an atom with a non-coulomb central field. part i. theory and methods. In *Mathematical Proceedings of the Cambridge Philosophical Society*, volume 24, pages 89–110. Cambridge university press, 1928.

[62] John Clarke Slater. The self consistent field and the structure of atoms. *Phys. Rev.*, 32(3):339, 1928.

[63] Torsten Fließbach. *Elektrodynamik: Lehrbuch zur Theoretischen Physik II*, volume 2. Springer-Verlag, 2012.

Bibliography

[64] John C Slater. Note on hartree's method. *Phys. Rev.*, 35(2):210, 1930.

[65] Vladimir Fock. Näherungsmethode zur lösung des quantenmechanischen mehrkörperproblems. *Zeitschrift für Physik*, 61:126–148, 1930.

[66] Max Born. Quantum mechanics of collision processes. *Zeit. Phys.*, 1926.

[67] Attila Szabo and Neil S Ostlund. *Modern quantum chemistry: introduction to advanced electronic structure theory*. Courier Corporation, 2012.

[68] Wolfram Koch and Max C Holthausen. *A chemist's guide to density functional theory*. John Wiley & Sons, 2015.

[69] LH Thomas. Lh thomas, proc. cambridge philos. soc. 23, 542 (1927). In *Proc. Cambridge Philos. Soc*, volume 23, page 542, 1927.

[70] Pierre Hohenberg and Walter Kohn. Inhomogeneous electron gas. *Phys. Rev.*, 136(3B):B864, 1964.

[71] Wolfram Koch and Max C Holthausen. *A chemist's guide to density functional theory*. John Wiley & Sons, 2015.

[72] Elliot H Lieb. Variational principle for many-fermion systems. *Phys. Rev. Lett.*, 46(7):457, 1981.

[73] Stefaan Cottenier et al. Density functional theory and the family of (l) apw-methods: a step-by-step introduction. *Instituut voor Kern-en Stralingsfysica, KU Leuven, Belgium*, 4(0):41, 2002.

[74] Walter Kohn and Lu Jeu Sham. Self-consistent equations including exchange and correlation effects. *Phys. Rev.*, 140(4A):A1133, 1965.

[75] Richard M Martin. *Electronic structure: basic theory and practical methods*. Cambridge university press, 2020.

[76] Eiji Nakamachi, Yasutomo Uetsuji, Hiroyuki Kuramae, Kazuyoshi Tsuchiya, and Hwisim Hwang. Process crystallographic simulation for biocompatible piezoelectric material design and generation. *Arch. Comput. Methods Eng.*, 20:155–183, 2013.

[77] Ulf Von Barth and Lars Hedin. A local exchange-correlation potential for the spin polarized case. i. *J. Phys. C: Solid State Phys.*, 5(13):1629, 1972.

Bibliography

[78] Robert G Parr. Density functional theory of atoms and molecules. In *Horizons of Quantum Chemistry: Proceedings of the Third International Congress of Quantum Chemistry Held at Kyoto, Japan, October 29-November 3, 1979*, pages 5–15. Springer, 1980.

[79] Alexander Khein, David Joseph Singh, and Cyrus J Umrigar. All-electron study of gradient corrections to the local-density functional in metallic systems. *Phys. Rev. B*, 51(7):4105, 1995.

[80] I Di Marco, J Minár, S Chadov, MI Katsnelson, H Ebert, and AI Lichtenstein. Correlation effects in the total energy, the bulk modulus, and the lattice constant of a transition metal: Combined local-density approximation and dynamical mean-field theory applied to ni and mn. *Phys. Rev. B*, 79(11):115111, 2009.

[81] Axel D Becke. Density-functional exchange-energy approximation with correct asymptotic behavior. *Phys. Rev. A*, 38(6):3098, 1988.

[82] AD Becke. Accurate local approximation to the exchange-correlation density functional: the mn12-l functional for electronic structure calculations in chemistry and physics. *Opt Phys*, 38:3098–3100, 1988.

[83] David C Langreth and MJ Mehl. Beyond the local-density approximation in calculations of ground-state electronic properties. *Phys. Rev. B*, 28(4):1809, 1983.

[84] Warren J Hehre. Ab initio molecular orbital theory. *Acc. Chem. Res.*, 9(11):399–406, 1976.

[85] P Perdew John, Chevary JA, Vosko SH, A Jackson Koblar, R Pederson Mark, Singh DJ, and Fiolhais Carlos. Erratum: Atoms, molecules, solids, and surfaces: Applications of the generalized gradient approximation for exchange and correlation. *Phys. Rev. B*, 48(7):4978–4978, 1993.

[86] Muhammad Ruhul Amin, Philipp Strobel, Amir Qamar, Tobias Giftthaler, Wolfgang Schnick, and Alexander Moewes. Understanding of luminescence properties using direct measurements on eu2+-doped wide bandgap phosphors. *Adv. Opt. Mater.*, 8(16):2000504, 2020.

Bibliography

[87] Somayeh Rastegar, Nasser L Hadipour, Hamed Soleymanabadi, et al. Theoretical investigation on the selective detection of so2 molecule by aln nanosheets. *J. Mol. Model.*, 20(9):1–6, 2014.

[88] Somayeh F Rastegar, Nasser L Hadipour, Mohammad Bigdeli Tabar, and Hamed Soleymanabadi. Dft studies of acrolein molecule adsorption on pristine and al-doped graphenes. *J. Mol. Model.*, 19(9):3733–3740, 2013.

[89] Denis Music, Richard W Geyer, and Jochen M Schneider. Recent progress and new directions in density functional theory based design of hard coatings. *Surf. Coat. Technol.*, 286:178–190, 2016.

[90] John P Perdew, Kieron Burke, and Matthias Ernzerhof. Generalized gradient approximation made simple. *Phys. Rev. Lett.*, 77(18):3865, 1996.

[91] Mosayeb Naseri, Dennis R Salahub, Shirin Amirian, Hatef Shahmohamadi, Mohammad Abdur Rashid, Mehrdad Faraji, and Negin Fatahi. Multi-functional lead-free ba2xsbo6 (x= al, ga) double perovskites with direct bandgaps for photocatalytic and thermoelectric applications: A first principles study. *Mater. Today Commun.*, 35:105617, 2023.

[92] Nor Diyana Abdul Aziz, Alyea Sofea Kamarulzaman, Norazila Ibrahim, and Zakiah Mohamed. Effect of mn doping on the optical and electrical properties of double perovskite sr2ticoo6. *Materials*, 15(15):5123, 2022.

[93] Ruosheng Zeng, Leilei Zhang, Yang Xue, Bao Ke, Zhuang Zhao, Dan Huang, Qilin Wei, Weichang Zhou, and Bingsuo Zou. Highly efficient blue emission from self-trapped excitons in stable sb3+-doped cs2naincl6 double perovskites. *J. Phys. Chem. Lett.*, 11(6):2053–2061, 2020.

[94] Saswata Halder, Ram Awdhesh Kumar, Ritwik Maity, and TP Sinha. A tailored direct-to-indirect band structure transition in double perovskite oxides influences its photocatalysis efficiency. *Ceram. Int.*, 49(5):8634–8645, 2023.

[95] Jiahe Lin, Tian Zhang, Bofeng Zhang, and Xiulin Wang. Wide-band-gaps two dimentional c3xn (x= n and p) for metal-free photocatalytic water splitting. *Appl. Surf. Sci.*, 542:148597, 2021.

[96] Akihide Iwase, Kenji Saito, and Akihiko Kudo. Sensitization of namo3 (m: Nb and ta) photocatalysts with wide band gaps to visible light by ir doping. *Bull. Chem. Soc. Jpn.*, 82(4):514–518, 2009.

Bibliography

[97] Tayebeh Ameri, Gilles Dennler, Christoph Lungenschmied, and Christoph J Brabec. Organic tandem solar cells: A review. *Energy Environ.*, 2(4):347–363, 2009.